

國立臺灣大學醫學院暨工學院醫學工程研究所



博士論文

Institute of Biomedical Engineering
College of Medicine and Engineering
National Taiwan University
Doctoral Dissertation

混合式骨減影頭部電腦斷層血管攝影及其臨床運用
Hybrid Bone Subtraction Head Computed Tomography
Angiography and Its Clinical Applications

李崇維

Chung-Wei Lee

指導教授：王兆麟 教授

Advisor: Jaw-Lin Wang, Ph.D.

中華民國 105 年 11 月

November 2016

致謝



本研究論文能完成要先感謝王兆麟教授及廖漢文教授的指導。王教授與生物力學實驗室提供假體平台，讓我對電腦斷層掃描下的移動所產生的變化能加以模擬，進而開發出適當的軟體解決問題，王教授也常提供不同的觀點，讓我在各方面都能做更多的思考。廖教授是我臨床及研究的老師，帶領我在臨床及研究上走出與眾不同的路。另外要特別感謝黃輝揚博士撰寫出優異的電腦程式，能將我天馬行空的想法化作現實。也要感謝林彥亨醫師提供統計上的諮詢。

感謝張允中教授在平時臨床及研究上的支持。感謝賴達明教授在臨床上對我的研究成果具有信心。感謝朱惟勤教授及王靖維教授百忙之中來擔任口試委員，並提供許多寶貴的意見，讓我受益良多。

最後要感謝我的家人，有老婆幫我打點家裡的一切，父母及岳父母在我忙碌的時候幫我帶小孩，讓我能持續往前。還有我兩個女兒，讓我明白不能輕易放棄，日後才能成為你們的榜樣。

中文摘要



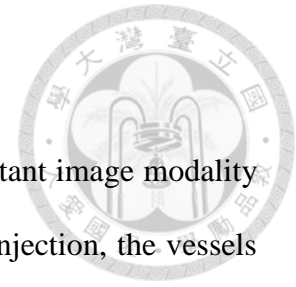
頭部電腦斷層血管攝影是臨床上常用來診斷許多血管異常及病變的重要工具，利用顯影劑的注射可以使得血管構造強烈顯影，進而評估其變化。骨頭在電腦斷層下亦為密度極高的構造，而頭部的血管會穿過骨頭而連接顱外與顱內血管，某些血管異常及病變恰巧發生在骨頭內的血管或是非常靠近骨頭的血管，這時使用傳統電腦斷層來評估血管將變得困難，影像的重組也會受到限制。

混合式骨減影頭部電腦斷層血管攝影是一種從電腦斷層影像中移除骨頭構造的方法，需要額外取得注射顯影劑前的影像。由於不同次掃描間通常會有些許位移，在骨減影之前須先進行位移校正，利用無顯影劑的影像取得骨頭的遮罩，在遮罩範圍內進行減影，並補上軟組織的密度值，即可得到一個消除骨頭後的電腦斷層影像。

利用混合式骨減影頭部電腦斷層血管攝影，原本會因為骨頭而影響診斷效果的疾病就有很高的機會可以在電腦斷層呈現。我們將之運用在兩種通常不會用電腦斷層來評估的腦血管疾病。其一是硬腦膜動靜脈瘻管，因為其發生位置緊鄰骨頭或在骨頭內，傳統電腦斷層不易偵測，但混合式骨減影頭部電腦斷層血管攝影卻得到很高的準確度，並且利於擬定血管內治療計畫。其二是頸動脈阻塞，阻塞段的遠端常位於顱底的骨頭內，傳統電腦斷層不易評估遠端位置，而利用混合式骨減影頭部電腦斷層血管攝影可以清楚的看到顱底段的阻塞位置，不同的阻塞位置，對於進行血管內重建的成功率及再阻塞率有顯著的差別。

關鍵詞：骨減影電腦斷層血管攝影、硬腦膜動靜脈瘻管、頸動脈阻塞。

Abstract



Head Computed Tomography Angiography (CTA) is an important image modality for evaluation of various vascular diseases of head. With contrast injection, the vessels become high-density structures and can be evaluated. The bones are also high-density structures on CT. Many head vessels traverse the bones. Some vascular anomalies or disorders occur in or adjacent to the bones, and conventional CTA is difficult to evaluate these situations. Image reconstruction is also not easy if the key structures are obscured by the bones.

Hybrid CTA is a technique for bone removal. An additional precontrast scan is needed. Motion correction between precontrast and postcontrast images is performed first. A bone mask is produced from precontrast images. Subtraction is performed inside the mask. A soft tissue value is added to the subtracted value for even background. A bone-eliminated CTA can be obtained.

With hybrid CTA, vascular diseases that may be masked by bones can be better evaluated. Here, hybrid CTA was used for two diseases. The first one was dural arteriovenous fistula (AVF), which was adjacent to or in the bones. Conventional CTA had limited value in diagnosis of dural AVF, but hybrid CTA showed a good accuracy. The other was carotid chronic total occlusion, with its distal end occasionally in the skull base. Hybrid CTA could detect the distal end of occlusion, which was associated with successful rate in endovascular recanalization and re-occlusion rate after recanalization.

Key words: Bone-subtraction computed-angiographic angiography, dural arteriovenous fistula, carotid occlusion.

目 錄



Chapter 1 Hybrid Subtraction Computed Tomography Angiography	1
1.1 Introduction.....	1
1.2 Image Acquisition.....	1
1.3 Image Processing	2
1.4 Impact of Hybrid Subtraction CTA	3
Chapter 2 Hybrid CTA in Diagnosis and Treatment Planning of Dural Arteriovenous Fistulas.....	12
2.1 Introduction.....	12
2.2 Materials and Methods.....	12
2.2.1 Patient and Control Populations.....	12
2.2.2 Image Evaluation.....	13
2.2.3 Treatment Planning	14
2.2.4 Statistical Analysis	14
2.3 Results.....	15
2.3.1 Patients	15
2.3.2 Imaging Analysis.....	15
2.4 Discussion	17
Chapter 3 Predicting Procedure Successful Rate and 1-Year Patency After Endovascular Recanalization for Chronic Carotid Artery Occlusion by CT Angiography	29
3.1 Introduction.....	29
3.2 Materials and Methods.....	31

3.2.1 Subjects	31
3.2.2 Patient Outcomes.....	32
3.2.3 Statistical Analysis	32
3.3 Results.....	32
3.4 Discussion.....	35
3.5 Conclusion	38
Chapter 4 Future Work.....	45
References	47



圖目錄



Figure 1-1: Subtraction CTA before and after registration (1).....	5
Figure 1-2: Subtraction CTA before and after registration (2).....	6
Figure 1-3: Generation of hybrid bone subtraction CTA after registration	7
Figure 1-4: Advantage of hybrid bone subtraction CTA	8
Figure 1-5: Different bone removal techniques of CTA in dural AVF.....	9
Figure 1-6: Illustration of intraosseous artery in carotid occlusion.....	10
Figure 2-1: Hybrid CTA findings in dural AVF.....	21
Figure 2-2: Intraosseous vessels in dural AVF and treatment	22
Figure 2-3: Relationship between dural AVF and normal veins.....	23
Figure 2-4: Hybrid CTA findings and special view for demonstration	24
Figure 3-1: Sub-classification of carotid occlusions and their outcomes.....	40
Figure 3-2: One-year patency after endovascular recanalization for chronic carotid artery occlusion in different groups.....	41

表目錄



Table 1-1: Acquisition Protocols of CT scanners	11
Table 2-1: Summary of 22 Patients with 24 Dural AVFs	25
Table 2-2: Diagnostic Performance of Imaging Signs at Hybrid CTA.....	26
Table 2-3: Interobserver Agreement in Reading Imaging Signs at Hybrid CTA.....	27
Table 2-4: Comparison of DSA with Readers for Grades Assigned to 24 Dural AVFs. 28	
Table 3-1: Demographics and clinical characteristics of all patients with chronic carotid occlusion.....	42
Table 3-2: Odds ratio for clinical predictors of stent occlusion in technically successful patients.....	43
Table 3-3: Univariable non-parametric survival analysis of clinical predictors for one-year stent patency.	44

Chapter 1

Hybrid Subtraction Computed Tomography Angiography

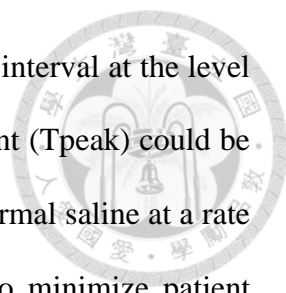


1.1 Introduction

Digital subtraction angiography (DSA), which is the standard for the diagnosis of intracranial vascular diseases, has a neurologic complication rate of 0.07%–1.3% [1,2]. Computed tomographic angiography (CTA) allows for rapid diagnosis and treatment decisions because acquisition of images is quick even in confused or uncooperative patients [3] and may be used as a first-line study in patients with acute ruptured cerebral aneurysm [4,5] and steno-occlusive diseases [6,7]. With algorithms for bone removal such as direct subtraction, local subtraction [8], and matched mask bone elimination (MMBE) [9], CTA provides even better image quality than standard CTA. The shortcomings of these various bone removal methods are complexity of use, operator dependence, high radiation dose, difficulties in differentiation of arterial loops or infundibula from the aneurysm, and the obscuring of an aneurysm in the cavernous internal carotid artery [9]. Hybrid CTA is a mixed bone subtraction and masking method for bone removal in CTA that can help demonstrate vessels close to or inside the skull bones.

1.2 Image Acquisition

Our routine CT angiographic protocol consisted of a combination of scanning before and after the administration of contrast material from the arch to the vertex (average, 32 cm) for direct subtraction. The acquisition protocol for each CT scanner is listed in **Table 1-1**. Twelve milliliters of contrast material (Ultravist 370; Bayer Schering Pharma, Berlin, Germany) was injected followed by 16 mL of normal saline at

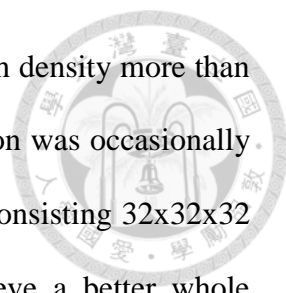


a rate of 4 mL/sec for a bolus test, which was scanned at a 2-second interval at the level of the ascending aorta so that the time required for peak enhancement (T_{peak}) could be obtained. Then, 60 mL of contrast material followed by 35 mL of normal saline at a rate of 4 mL/sec was injected for the CT angiographic acquisition. To minimize patient movement, the precontrast scan was obtained simultaneously during contrast material injection, and the postcontrast scan was obtained after a delay (T_{delay}). The acquisition time plus the T_{delay} was equal to $T_{\text{peak}} + 4$ to 8 seconds according to the table speed to obtain an early venous phase at the level of skull base. Normal venous structures at skull base level should be faintly enhanced for better evaluation of arteries and veins.

The peak tube voltage (KVp) was 100KV rather than routine 120KV in our protocol for each scanner. For the same tube current, decrease of KVp from 120KV to 100KV resulted in about 1/3 dose reduction with acceptable contrast to noise ratio. The reduced dose was shift to the pre-contrast scan, which had half radiation dose of the post-contrast scan. This protocol did not increase the overall radiation doses of the patients. However, with the pre-contrast images, bone removal could be easily performed by software.

1.3 Image Processing

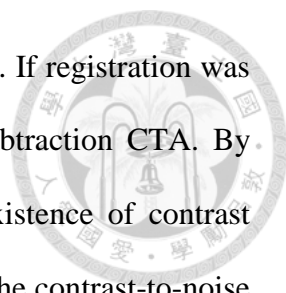
Using our subtraction CTA protocol, the result of direct subtraction could be adequate if the patient did not have motion during scanning. However, in most cases, registration for precontrast and postcontrast images should be performed first (**Figure 1-1**). The source images were transferred to a personal computer with operating system of Windows 7. A home-made prototype program written on Matlab was used. Precontrast and postcontrast directories were selected, and the result would be saved in



a new assigned directory. We used a rigid registration for pixels with density more than 150 Hounsfield Unit (HU). However, whole volume rigid registration was occasionally unsatisfactory. The whole volume was separated into many cubes consisting 32x32x32 pixels. Each cube was further registered in local region to achieve a better whole volume registration. After whole volume registration, the bones could be subtracted almost completely (**Figure 1-2**). Then, a mask was produced by using a threshold level of 150 HU in the precontrast images. The mask was slightly widened by means of dilation [10] with 1 pixel, as suggested in the original MMBE method [11], to allow for partial volume effects and slight mismatch between registered precontrast and postcontrast images. We performed subtraction in the masking area. Subtraction was sensitive to mis-registration, and our registration method could usually achieve the requirement. The postcontrast images were processed according to the mask: In the masking area, the value was defined as the postcontrast value minus the precontrast value plus 40 HU; out of the masking area, only the postcontrast value was preserved. The purpose of adding 40 HU was to make a background similar to that of the soft tissue (soft tissue compensation) (**Figure 1-3**). The processed images were transferred to the workstation (Advanced Workstation 3.1, GE Healthcare) for reconstruction and evaluation.

1.4 Impact of Hybrid Subtraction CTA

Recently, many bone removal techniques, including direct subtraction CTA, and MMBE CTA, were developed for diagnosing cerebral aneurysms. In the algorithm of MMBE CTA, the transosseous or intraosseous vessels will be masked and become poorly visualized because partial volume effect and the dilation operation could change the vessel pixels (which touching the bone) into mask during processing. MMBE CTA



could obliterate minor mis-registration artifacts within the bone area. If registration was not perfect, the result of MMBE CTA would look better than subtraction CTA. By using direct subtraction CTA, one can obtain an image of the existence of contrast material (similar to DSA) that can be used for diagnosis. However, the contrast-to-noise ratio decreases, especially when a low-dose precontrast scan is used for masking. MMBE CTA removes bone, as well as adjacent tissues, which are frequently affected by certain vascular disorders. Vessels traversing in or on the bones may also be eliminated. Our hybrid technique can be used to perform subtraction in the masked area and can keep postcontrast image data out of the masked area. (**Figure 1-4, Figure 1-5**)

Hybrid CTA has the advantage of demonstrating the transosseous or intraosseous vessels. (**Figure 1-6**) This makes diagnosis of vascular diseases in or adjacent to the bones possible. Hybrid CTA can provide a rapid diagnosis in many clinical situations because of its quick acquisition and non-invasive nature.

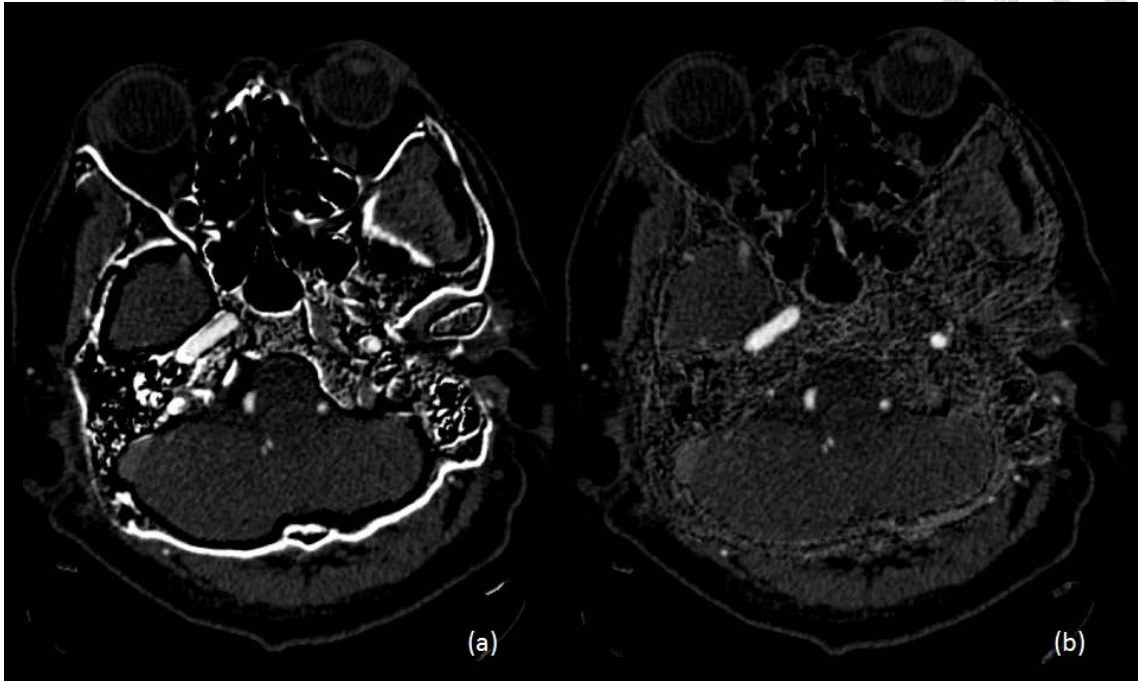


Figure 1-1: Hybrid bone subtraction without registration (a) and after registration (b).

Mis-registration artifacts decreased significantly.

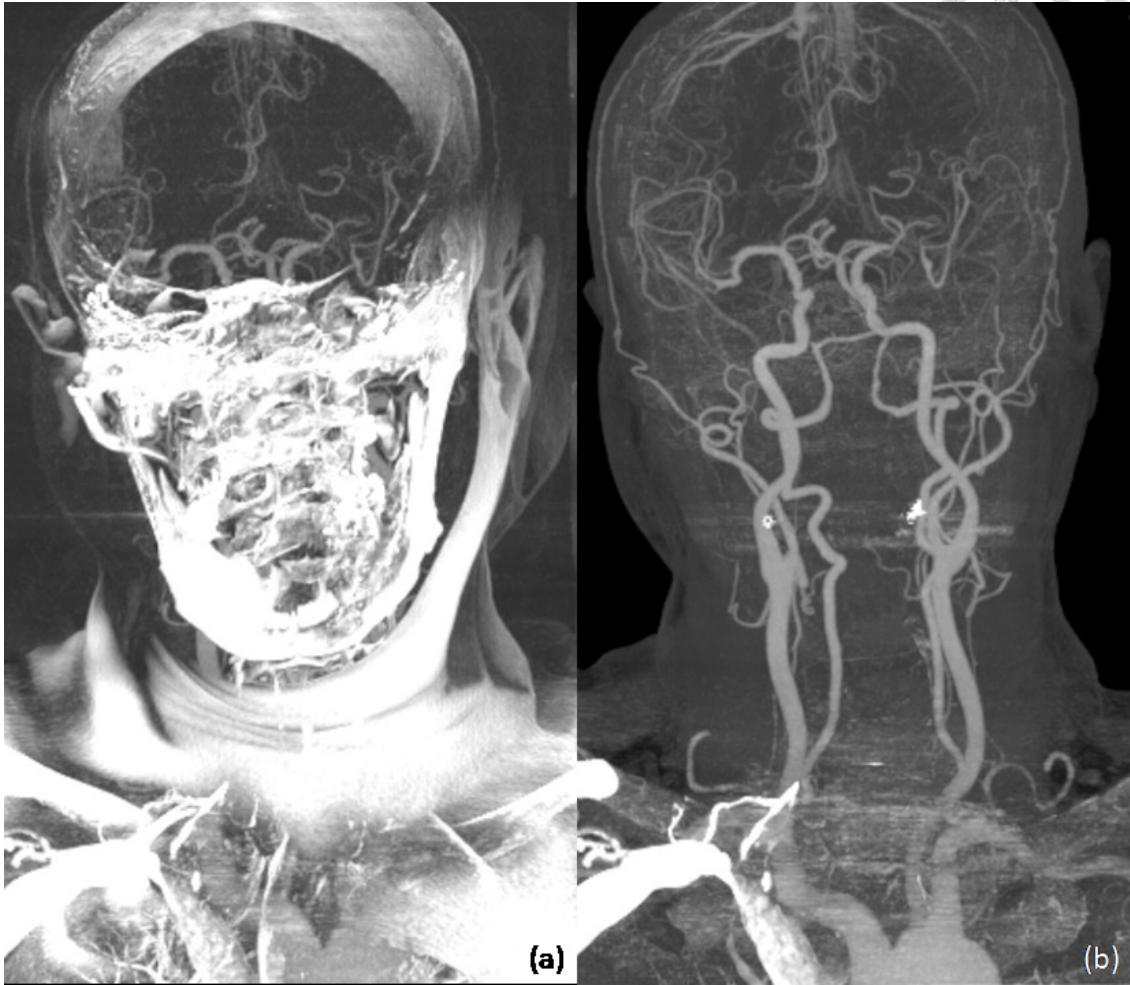


Figure 1-2: Thick maximal intensity projection (MIP) of subtraction CTA (a) without bone registration (b) with bone registration. The image quality improves after bone registration.

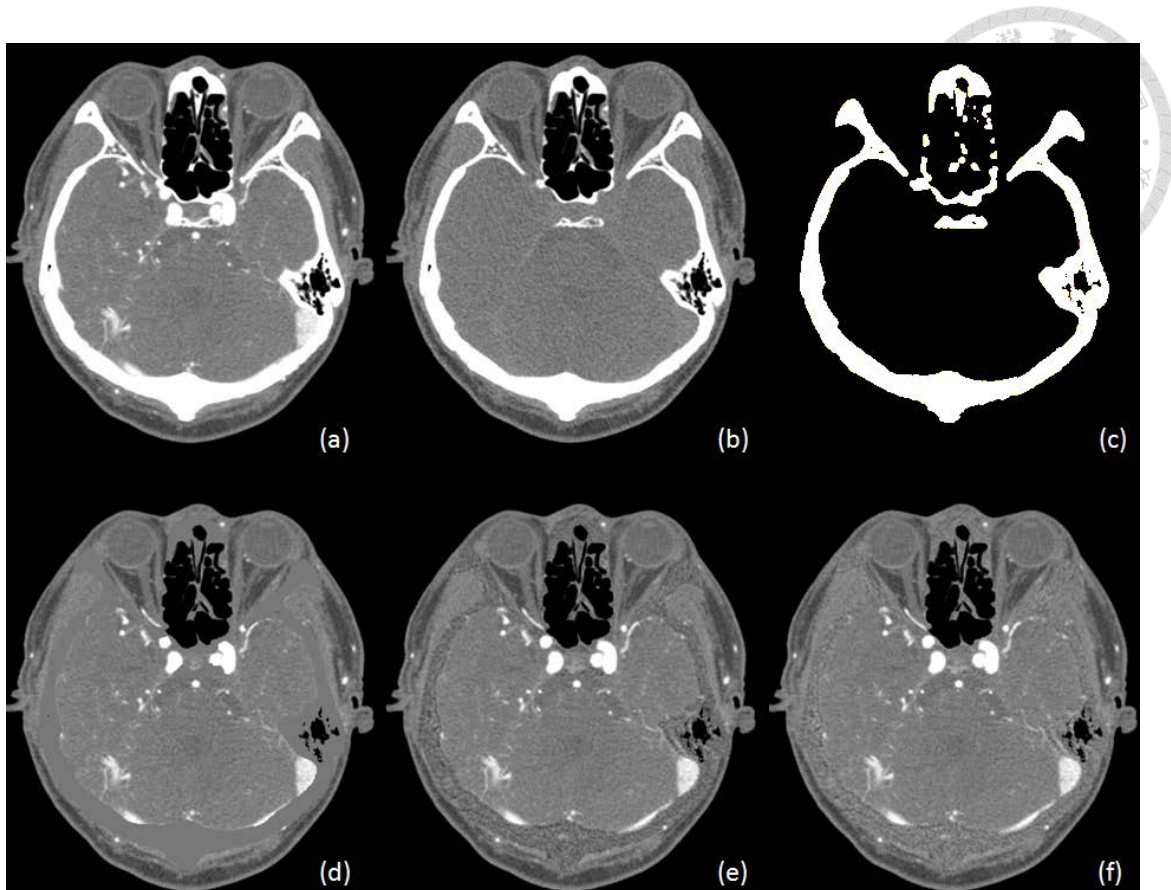


Figure 1-3: Generation of hybrid bone subtraction CTA after registration. (a) Postcontrast image (CTA). (b) Precontrast image. (c) Bone mask generated from precontrast image by threshold ($>150\text{HU}$) and 1-pixel dilatation. (d) MMBE image from CTA with soft tissue value (40HU) in bone mask. (e) Hybrid bone subtraction CTA with simple subtraction in the mask, resulting in lower density in the bone. (f) Hybrid bone subtraction CTA with soft tissue compensation to achieve an even background.

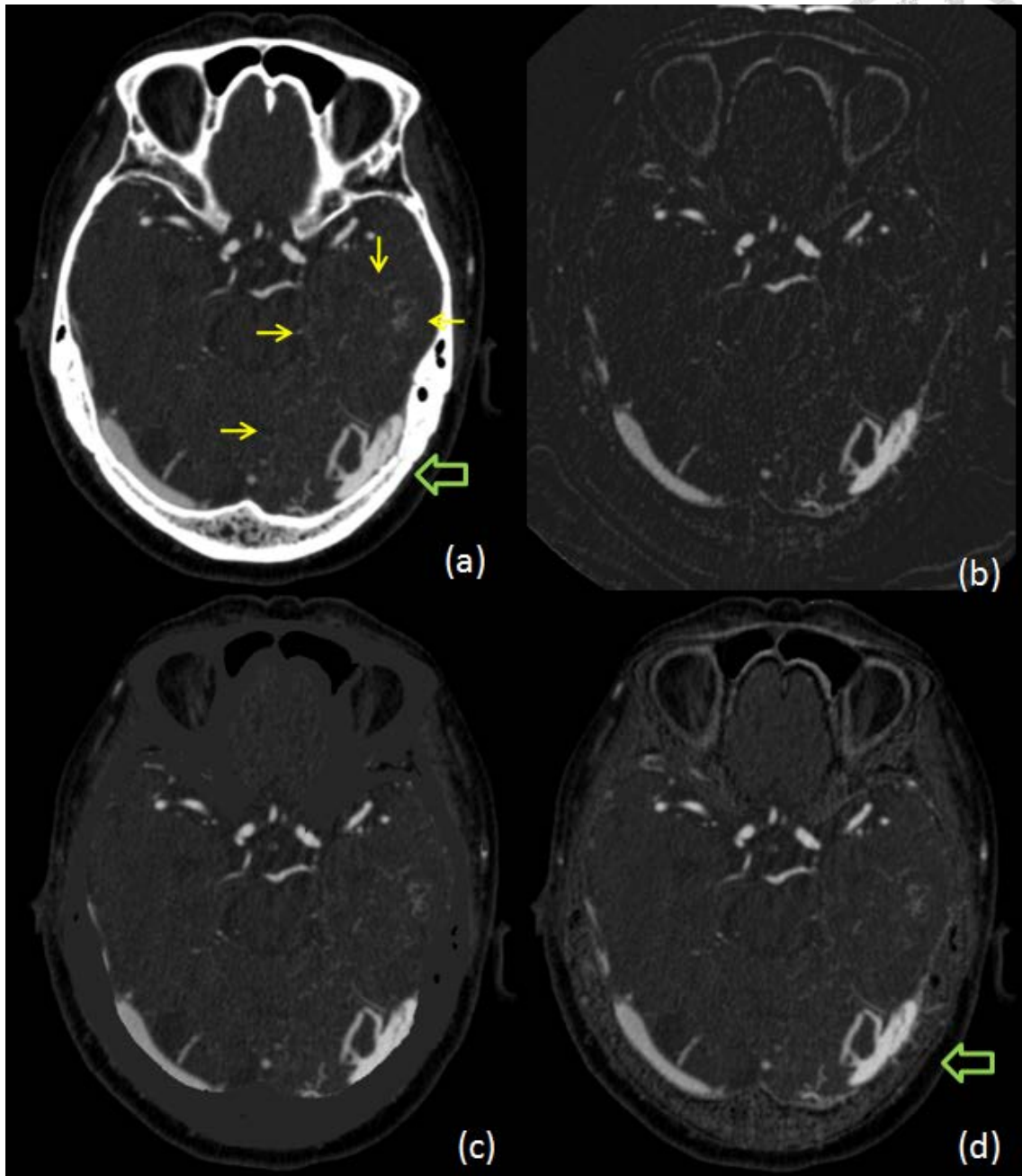


Figure 1-4: Advantage of hybrid bone subtraction CTA (hybrid CTA) (a) unprocessed CTA image showed early enhancing isolated left transverse sinus (large arrow) and multiple engorged medullary veins in left temporal lobe and left cerebellum (surrounded by small arrows). (b) subtraction CTA increased noises in the brain parenchyma, the engorged medullary veins were masked by noise. (c) MMBE CTA masked the information in and adjacent to bones. (d) hybrid CTA preserved the information in brain parenchyma, and added information in the bones (large arrow).

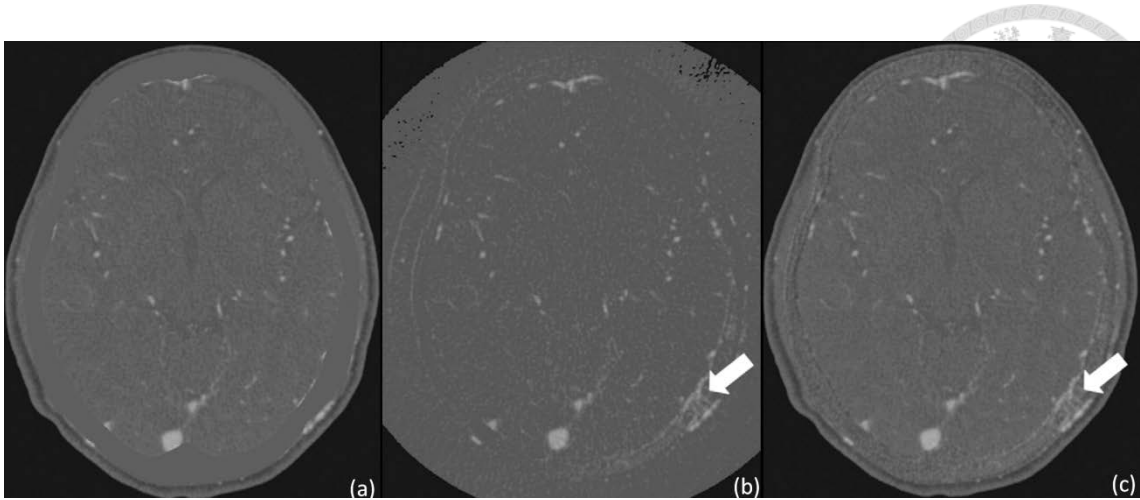


Figure 1-5: Images in 60-year-old man with pulsatile tinnitus. Images were obtained with **(a)** MMBE, **(b)** direct subtraction, and **(c)** hybrid subtraction (hybrid CTA). **(b, c)** Arrow = prominent transosseous arteries supplying the arteriovenous fistula. Tiny channels in the bone can be seen; these arteries are not seen on **(a)**. Higher image noise can be seen on **(b)**. In this case, hybrid CTA on **(c)** outlined the abnormal vessels best.

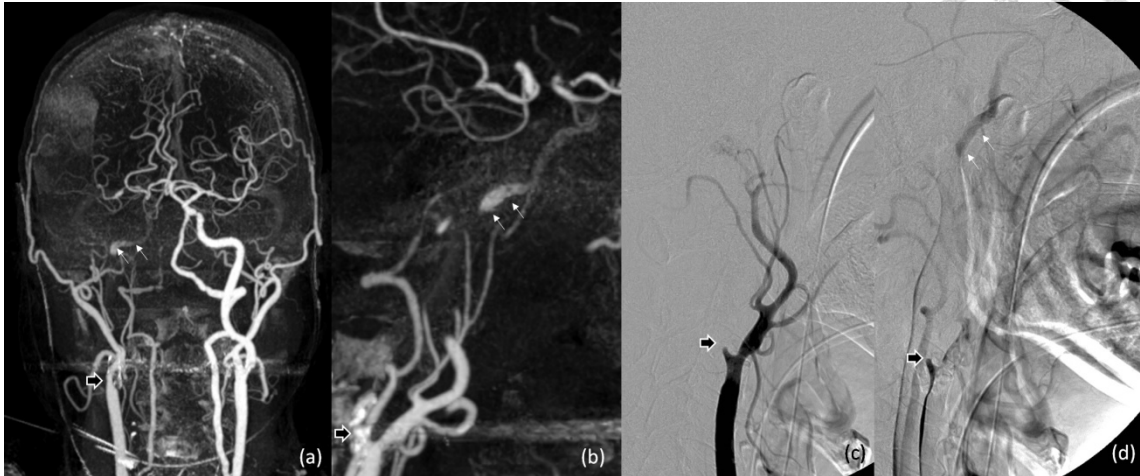


Figure 1-6: Maximal intensity projection (MIP) of hybrid CTA in frontal projection (a) and lateral projection (b). Lateral projection of right carotid angiography at early arterial phase (c) and late arterial phase (d). Black arrow indicated the occlusion point of proximal internal carotid artery (ICA). White arrows indicated reconstitution of petrous segment of ICA, which was clearly seen on hybrid CTA.

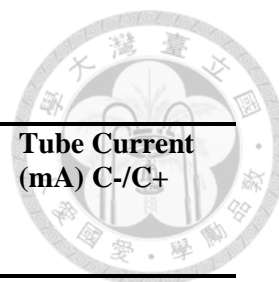


Table 1-1: Acquisition Protocols of CT scanners

CT scanner	Collimation (mm)	Pitch	Rotation (sec)	KVp (kV)	Tube Current (mA) C-/C+
GE Lightspeed VCT (before 2010)	32x0.625	0.969	0.4	100	200/400
GE Lightspeed VCT (after 2010)	64x0.625	0.984	0.4	100	200/400
Siemens Sensation 64	64x0.6	0.8	0.33	100	243/484
Philips Ingenuity CT	64x0.625	1.015	0.4	100	100/250

KVp: Kilovoltage peak. C-: precontrast. C+: postcontrast.

Chapter 2

Hybrid CTA in Diagnosis and Treatment Planning of Dural

Arteriovenous Fistulas



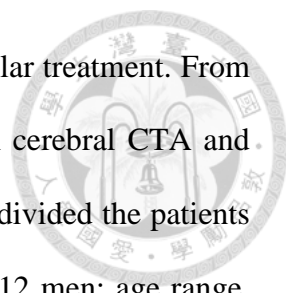
2.1 Introduction

Dural arteriovenous fistulas (AVFs) occur at dural sinuses, which are proximate to or inside the skull bones. Because of the overlapping bone structures, it is difficult to demonstrate the detailed vascular pattern and to make a diagnosis of dural AVF with conventional CTA, especially in small lesions. Magnetic resonance (MR) imaging and MR angiography were thought to be more useful in the diagnosis of dural AVF [12-14], but they cannot be used in patients with a non-MR-compatible pacemaker or in uncooperative patients. To our knowledge, the use of CTA for the diagnosis of dural AVF remains uncommonly reported. A hybrid CTA can help demonstrate vessels close to or inside the skull bones that makes diagnosis of dural AVF possible. The purpose of this study was to analyze the diagnostic effectiveness and application of CTA by using hybrid CTA algorithm in dural AVFs.

2.2 Materials and Methods

2.2.1 Patient and Control Populations

This study was approved by our institutional review board. In this study, the comparison between hybrid CTA and DSA, the determination of the presence of specific imaging signs for diagnosis of dural AVFs at hybrid CTA, and the test of inter-observer agreement were performed retrospectively. However, we used hybrid



CTA in treatment planning before the patients underwent endovascular treatment. From January 1, 2008, to March 31, 2009, 167 patients underwent both cerebral CTA and DSA in National Taiwan University Hospital (Taipei, Taiwan). We divided the patients into two groups: patients with a dural AVF (n=22, 10 women and 12 men; age range, 41–77 years; mean age, 60.3 years \pm 11.3) and patients without a dural AVF, the control group. The control group (n=14, six female and eight male subjects; age range, 17–77 years; mean age, 61.9 years \pm 17.1) included patients who did not have any cerebrovascular abnormalities noted at DSA; patients excluded from the control group included those with cerebral arteriovenous malformation (n=3), those with aneurysm (n=59), those with direct carotid artery–cavernous fistula (n=6), those with cerebral space-occupying lesions (n=2), those with dural sinus thrombosis (n=3), those with moyamoya disease (n=6), those with a large stroke (n=48), and those who had undergone external carotid artery–internal carotid artery bypass surgery (n=4).

2.2.2 Image Evaluation

Identification information was removed from the hybrid CT angiographic source images and maximum intensity projection images, and the images were evaluated independently by two neuroradiologists who were blinded to the clinical data and results of diagnostic CT and DSA. The methods of interpretation included multiplanar reformation (MPR), maximum intensity projection (MIP), and volume rendering. The comparison between hybrid CTA and DSA, the determination of presence of imaging signs for diagnosis of dural AVFs, and the test of inter-observer agreement were performed retrospectively with high-brightness liquid crystal display monitors (3 megapixels, 1536 \times 2048 native resolution, monochrome). From the final post-processed images, the readers recorded the presence and location (left side, right

side, or midline) of dural AVFs and the presence of imaging signs, including engorged arteries, transosseous enhanced vessels, engorged extracranial veins, engorged cortical veins, asymmetric sinus enhancement, and the associated dural sinus occlusion. We assigned grades to the dural AVFs by using the system proposed by Cognard et al [15]. DSA images were used as the reference standard.

2.2.3 Treatment Planning

The treatment was planned according to the grade of dural AVF. In our institution, transvenous embolization was the method of choice for treating dural AVFs if there was no normal cortical vein draining into the lesion sinus and the lesion sinus was accessible. We used all available imaging data for treatment planning, including images from hybrid CTA, DSA, and MR angiography. Treatment planning with hybrid CTA was performed before the patients received endovascular treatment. We applied the imaging data to analyze the best route to approach the point of the fistula. We usually designed two routes for the transvenous approach for each case. In those patients with an occluded sinus, we always tried to cross the occluded access site. If the transvenous approach failed or preservation of normal cortical venous drainage was technically difficult, we changed the treatment to transarterial embolization (eg, occlusion of the feeder vessels and fistulas with liquid embolic material or applying coils to the fistula after accessing the fistula from the arterial route).

2.2.4 Statistical Analysis

We compared the imaging findings and grades of dural AVF obtained with hybrid CTA with those obtained with DSA. Sensitivity, specificity, positive predictive value, and negative predictive value were calculated for the six CT angiographic imaging

findings (engorged artery, transosseous enhanced vessels, engorged extracranial vein, engorged cortical vein, asymmetric sinus enhancement, and dural sinus occlusion) individually and overall. The adjusted Wald method was used to estimate the 95% confidence intervals (CIs) of observed rates. The Cohen un-weighted κ statistic was used to assess the level of inter-observer agreement with regard to imaging signs for diagnosis of dural AVFs seen with hybrid CTA. A value of less than 0.20 implied poor agreement; values of 0.21–0.40, fair agreement; values of 0.41–0.60, moderate agreement; values of 0.61–0.80, substantial agreement; and values of 0.81–1.00, almost perfect agreement [16]. The 95% CI and Cohen κ were computed with online calculators [17,18].

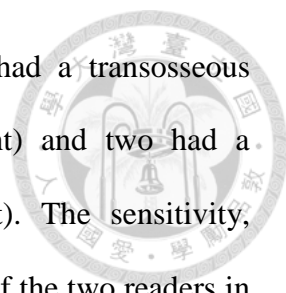
2.3 Results

2.3.1 Patients

Of 22 patients, two (patients 8 and 10) had two dural AVFs each; thus, there were a total of 24 dural AVFs. **Table 2-1** lists the demographic information, clinical manifestations, lesion locations, treatments, and outcomes for the 22 patients with 24 dural AVFs. There was no significant difference in age distribution ($P=0.579$) and birth sex ($P=0.728$) between the control subjects and patients with dural AVF.

2.3.2 Imaging Analysis

All 24 dural AVFs were examined with DSA and hybrid CTA. In all 24 lesions, at least two of the six imaging signs were present (**Figure 1-5, Figure 2-1**). Overall, the most common imaging finding was asymmetric sinus enhancement; this was not present in only the two patients with a dural AVF in the superior sagittal sinus. In the control

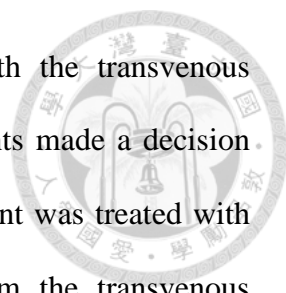


group, three subjects had a false-positive finding (two patients had a transosseous enhanced vessel, one patient had asymmetric sinus enhancement) and two had a false-negative finding (both had asymmetric sinus enhancement). The sensitivity, specificity, positive predictive value, and negative predictive value of the two readers in consensus are listed in **Table 2-2**. The κ test (**Table 2-3**) revealed a high level of interobserver agreement in the reading of the imaging signs. The best agreement was in regard to sinus occlusion and asymmetric sinus enhancement, followed by transosseous enhanced vessels.

As compared with the grade assigned with DSA (**Table 2-4**), the observed agreement between DSA and the readers was 100% for cavernous sinus, hypoglossal, and clival lesions and 78%–89% for lesions in the transverse sigmoid sinus.

2.3.3 Treatment Planning

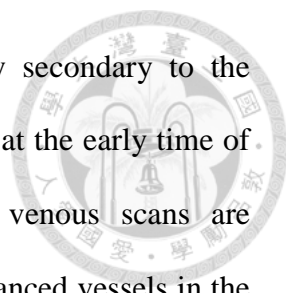
Treatment planning by using hybrid CTA was performed before the patients received endovascular treatment. Hybrid CTA can provide additional information in identifying the best route of approach to treat the dural AVF. In osteodural type dural AVFs, the pathway between the drained sinus and the fistula is very tortuous and small. Hybrid CTA can provide the road map about the best route to approach the lesion (**Figure 2-2**). In those dural AVFs that involved only the dura mater, hybrid CTA can localize exactly the fistula site inside the dura mater and its relationship to adjacent normal cerebral venous drainage and sinus (**Figure 2-3**). Hybrid CTA can also provide a high-resolution birds-eye view of the dural AVFs (**Figure 2-4**), which cannot be obtained with DSA. Although the drained sinus of the dural AVF was occluded, hybrid CTA can provide the information about localization and pathway for the trial to cross the occluded sinuses. In this series, nine patients were treated with the transvenous



approach, seven patients who were originally to be treated with the transvenous approach were treated with the transarterial approach, seven patients made a decision not to receive any treatment during the study period, and one patient was treated with stereotactic radiosurgery (**Table 2-1**). All nine patients in whom the transvenous approach was used were treated by using a route planned according to the results of hybrid CTA. In the patients who finally were treated with the transarterial approach (**Figure 2-4**), either treatment failed with the transvenous route or use of this route was not safe.

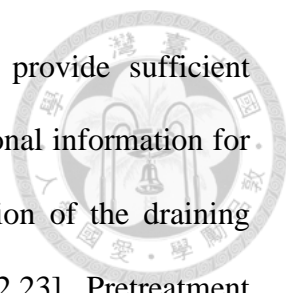
2.4 Discussion

The difficulty of bone removal limits the application of CTA in the diagnosis of dural AVF. In one recent report [19], CTA had a sensitivity of 15.4% in the diagnosis of dural AVF. In our study, we proved that hybrid CTA is a promising tool for the diagnosis of dural AVF. DSA can help in the diagnosis of dural AVF, can depict the supplying arteries, and can aid characterization of the draining system of dural AVF. The latter determines the clinical presentation, grade, and therapeutic strategy in patients with a dural AVF [15,20,21]. Our results suggest that hybrid CTA could be used to determine the diagnosis in all types and grades of dural AVFs, to demonstrate the feeder artery, to aid localization of the lesion, and to show the pattern of venous drainage. One patient in the control group had a false-positive sign of asymmetric early venous enhancement. From DSA, we found that the patient had dominant drainage of the superior sagittal sinus to the right transverse sinus, which was less enhanced compared with the left side at hybrid CTA. We speculate that the vein of Labbé was diluted more at the dominant right transverse sinus owing to nonopaque blood flow coming from the superior sagittal sinus. Asymmetric opacification of the transverse and



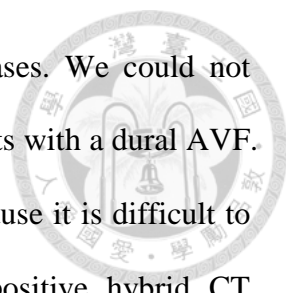
sigmoid sinuses during CTA is a rather common finding, likely secondary to the preferential direction of opacified blood flow to the dominant sinus at the early time of arterial scanning. This asymmetry disappears when late-phase venous scans are obtained. Two patients had a false-positive sign of transosseous enhanced vessels in the occipital bone near the sigmoid sinus. We speculate that these were emissary veins. We were not able to identify the direction of the vessels inside the cranium with hybrid CTA. We need to emphasize that finding at least two imaging signs present is the key to making the right diagnosis in dural AVFs.

Two patients with a dural AVF in the superior sagittal sinus did not have asymmetric sinus enhancement. In general, the vertex superior sagittal sinus becomes densely enhanced near the end of the scan. As such, enhancement asymmetry may not be apparent in a patient with a dural AVF at or close to the vertex superior sagittal sinus. However, other signs allowed diagnosis of dural AVF even in these patients with dural AVF of the superior sagittal sinus. Dural AVFs can be divided into two major groups according to their locations: cavernous sinus and non-cavernous lesions. In cavernous sinus dural AVFs, frequent findings include asymmetric early sinus enhancement and engorgement of the extracranial veins (frequently superior ophthalmic veins). Engorged arteries are infrequently seen in cavernous sinus dural AVFs because of their relatively small size. In non-cavernous dural AVFs, engorged arteries are more frequently seen. Engorgement of cortical veins and extracranial veins depend on the size and the drainage patterns of the dural AVF. On the basis of our results, hybrid CTA is highly sensitive for different types of dural AVFs, especially in patients with the osteodural-type lesion. Hybrid CTA has the advantage of demonstrating the transosseous vessels and also the fistula inside the bone structures.



On the basis of our study results, hybrid CTA may also provide sufficient information for treatment planning. Hybrid CTA can provide additional information for identifying the route of approach to treat dural AVFs. Identification of the draining venous pattern is important for the treatment of dural AVFs [22,23]. Pretreatment planning with hybrid CTA was feasible in our series. Transvenous embolization is one of the treatments of choice for most dural AVFs. Hybrid CTA can be used to eliminate the bone structure, while the image noise in non-bone areas is not increased, and to obtain better three-dimensional volume data.

Our study had limitations. Because this was a retrospective study, the tube current for precontrast scanning could only be reduced by half. The radiation dose for precontrast scanning was slightly higher than that in the scanning protocol recommended for MMBE CTA, in which one-quarter tube current is suggested for a precontrast scan. The effective tube current–time product used in our hybrid CT angiographic scanning protocol was similar to that used in a study on the use of MMBE study [24]; however, the tube voltage is 100 kVp rather than 120 kVp in the proposed hybrid CTA protocol. For example, with the same machine (scanner B in our study) and same irradiated length, the irradiation dose (estimated CT dose index volume) was 9.4 mGy for the precontrast scans and about 18.8 mGy for the post-contrast scans with the hybrid CTA protocol and 7.8 mGy and 28.1 mGy, respectively, in the other MMBE protocols [24]. So, the total irradiation dose is lower with hybrid CTA than with other MMBE methods. A lower peak kilovolt is not used because of the concern about contrast-to-noise ratio on the images.



Another limitation of our study was the small number of cases. We could not conclude that hybrid CTA can be used for the diagnosis in all patients with a dural AVF. False-positive and false-negative rates may be under-estimated because it is difficult to have a large number of patients who undergo DSA without positive hybrid CT angiographic, MR imaging, or MR angiographic findings. In addition, we used subjective findings that have not been well established for diagnosing retro-grade cortical veins. These need to be better defined with further research. In conclusion, we found that hybrid CTA is a valuable tool for the diagnosis of dural AVF. It can provide the key information necessary for treatment planning. Further studies in larger series of patients are warranted.

Note:

This part was published on *Radiology* 2010.

Lee CW, Huang A, Wang YH, Yang CY, Chen YF, Liu HM. Intracranial Dural Arteriovenous Fistulas: Diagnosis and Evaluation with 64-Dector Row CT Angiography. *Radiology*. 2010; 256: 219-228.

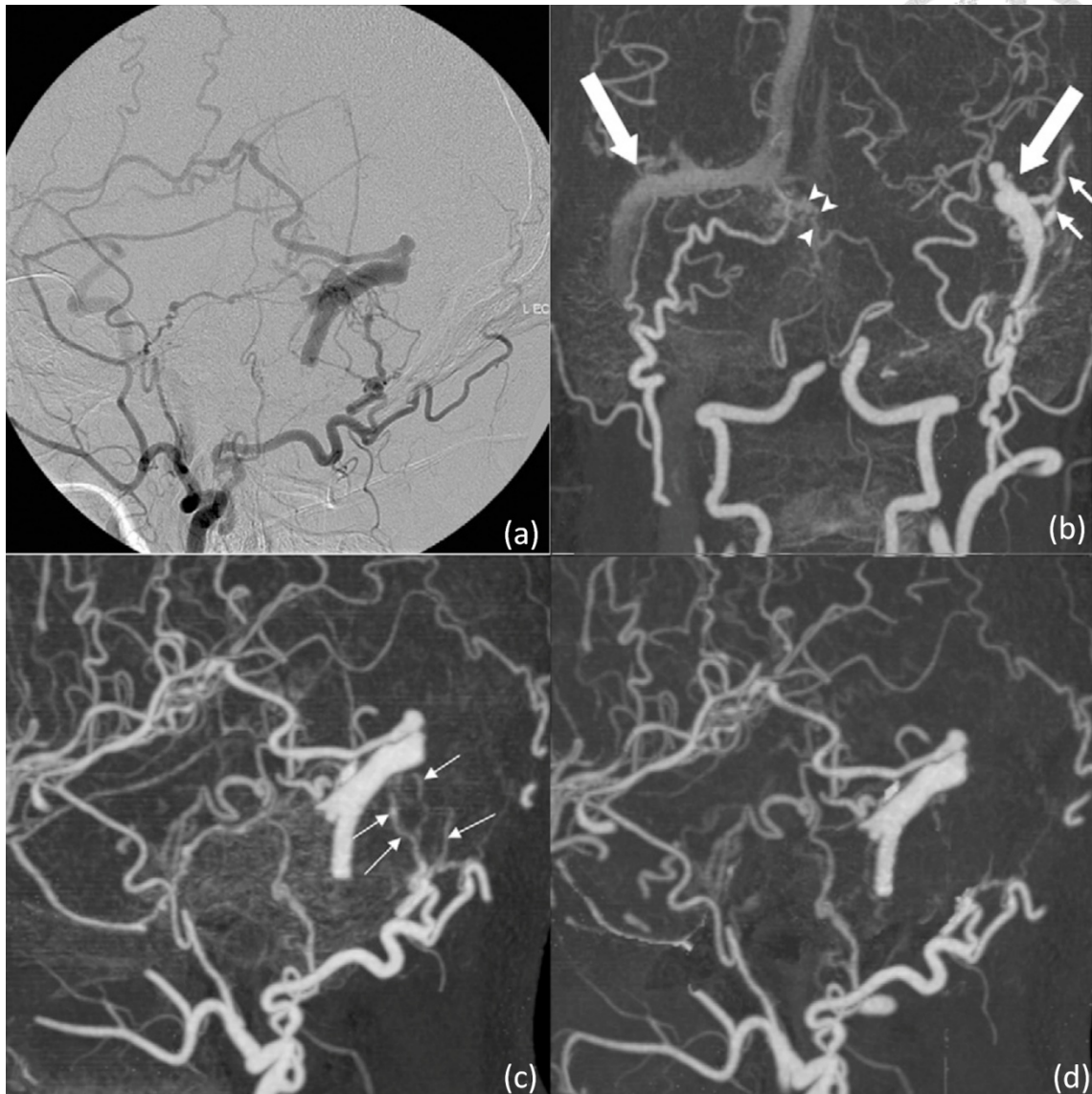


Figure 2-1: Patient 8. (a) Lateral DSA image after left external carotid injection shows isolated left transverse sigmoid sinus dural AVF. (b) Coronal hybrid CT angiogram shows asymmetric sinus enhancement (large arrows), engorged cortical veins (small arrows), and incidental small right proximal transverse sinus dural AVF (arrowheads). Images from (c) hybrid CTA and (d) MMBE CTA show isolated, occluded transverse sinus. Transosseous enhanced vessels (arrows on c) could be demonstrated only on hybrid CT angiogram.

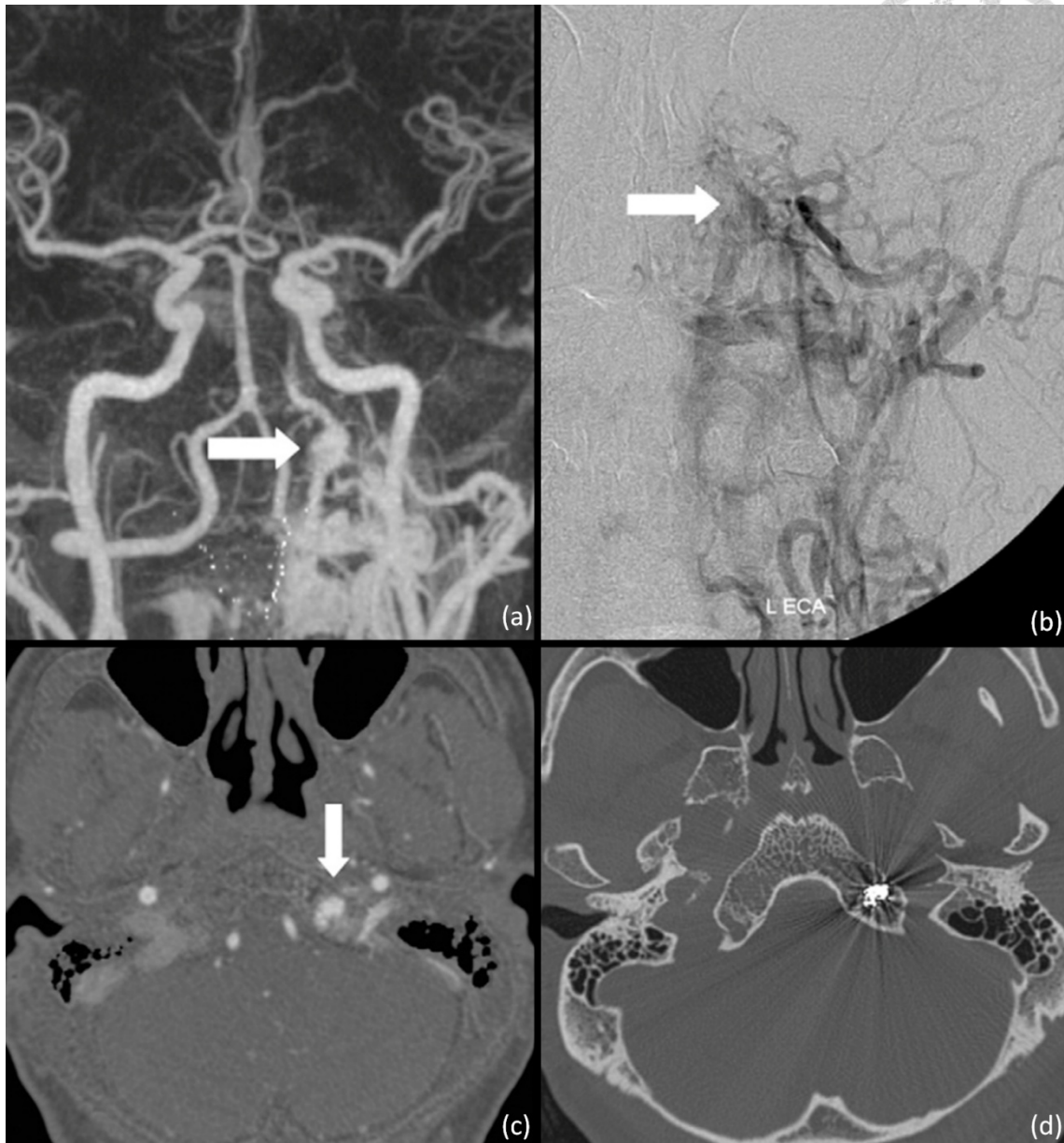


Figure 2-2: Patient 15. Images in 48-year-old man with pulsatile tinnitus and dizziness.

(a) Maximum intensity projection image from hybrid CTA shows dural AVF (arrow) with early enhancement and engorged drainage vein at the left clivus to the paraspinal area. (b) hybrid CTA source image shows fistula in the left clivus (arrow). (c) DSA image of left external carotid artery (L ECA) demonstrates a fistula (arrow) at the left hypoglossal-clival area with paraspinal drainage. The lesion was treated with the transvenous approach according to findings from hybrid CTA through the route of the anterior internal spinal venous plexus. (d) Precontrast image obtained after embolization shows coils inside left clivus.

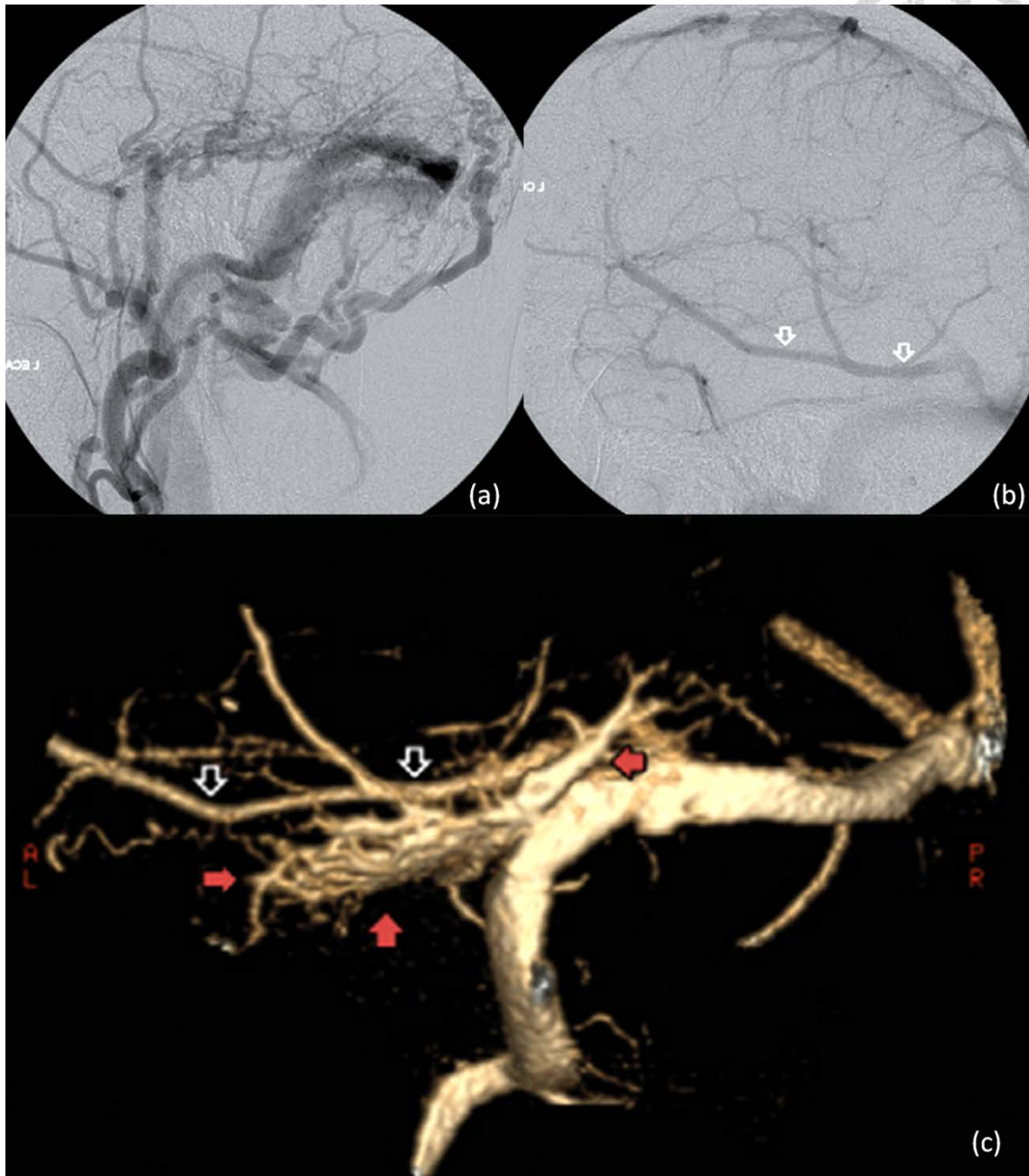


Figure 2-3: Patient 13. Images in 60-year-old man with pulsatile tinnitus. (a) Lateral projection of left external carotid artery demonstrates a type IIA dural AVF (Cognard et al [4] classification) at the left transverse-sigmoid sinus area. (b) Left common carotid artery angiogram obtained in the venous phase shows the left vein of Labbé (arrows) also draining into the left transverse sinus. (c) Hybrid CT angiogram obtained with volume rendering shows the fistula (red arrows) actually located at the dura next to the sigmoid sinus. The vein of Labbé (open arrows) is next to the fistula and drains into the transverse sinus.

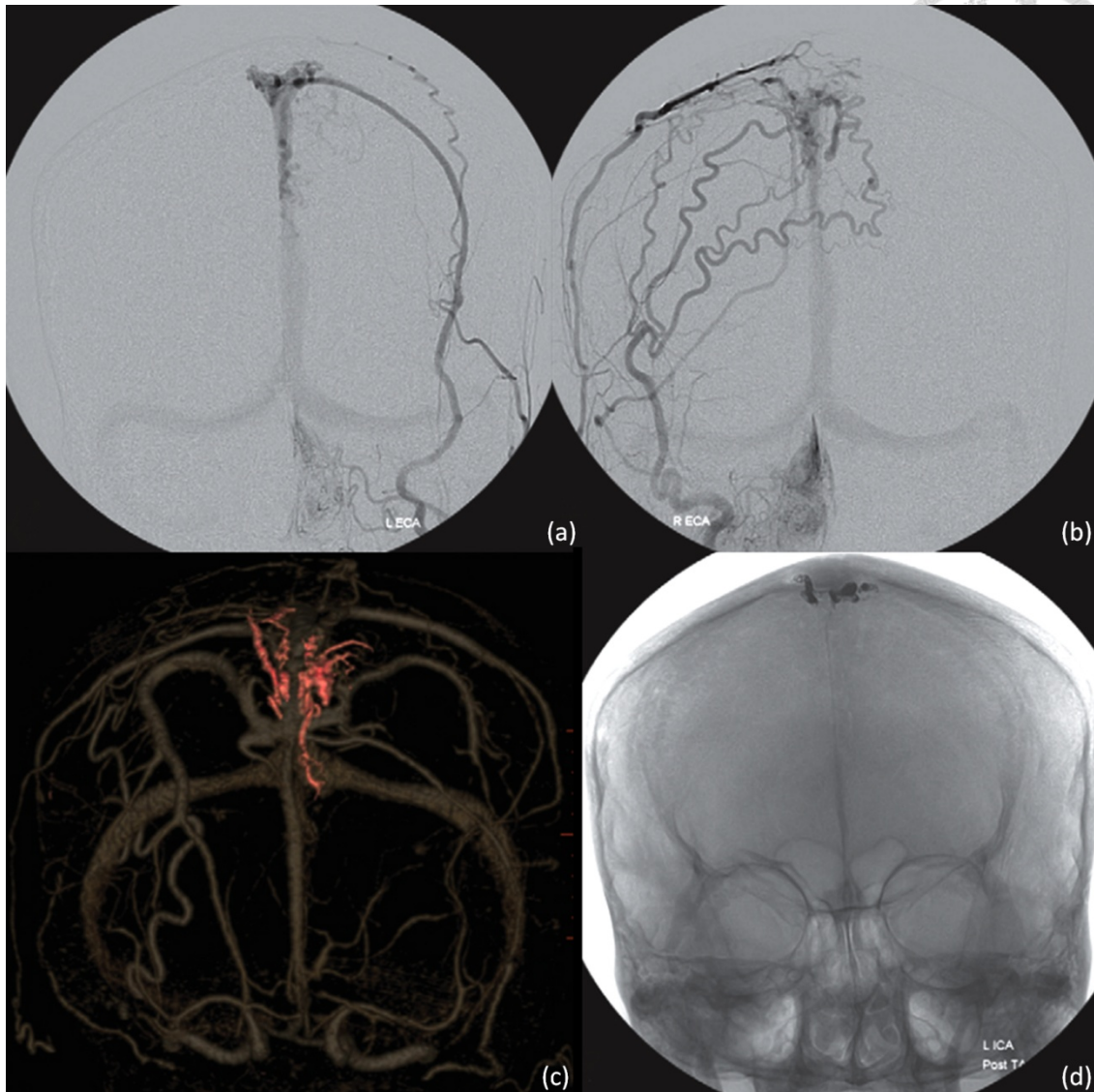


Figure 2-4: Images in 56-year-old woman with pulsatile tinnitus. (a, b) DSA images of bilateral external carotid arteries demonstrate the fistula, engorged cortical vein, and superior sagittal sinus. The relationship between the fistula and the superior sagittal sinus is not clearly shown. (c) Hybrid CT angiogram obtained with volume rendering depicts the fistula inside the bilateral paramedian posterior frontal bones (red), the engorged cortical drainage vein (red), and patent superior sagittal sinus. After transarterial approach with coils deploying in the venous side of the fistula, complete obliteration of the lesion was achieved. (d) Plain radiograph shows platinum coils inside the bilateral paramedian posterior frontal bones.

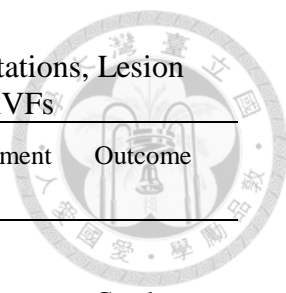


Table 2-1: Summary of Demographic Information, Clinical Manifestations, Lesion Locations, Treatments, and Outcomes in 22 Patients with 24 Dural AVFs

Patient No./Sex/Age(y)	Location	Clinical Manifestation	Treatment	Outcome
Cavernous sinus				
1/M/60	CS	Chemosis	TAE	Good
2/M/65	CS	Ophthalmoplegia	TVE	Good
3/F/68	CS	Chemosis	TVE	Good
4/F/69	CS	Chemosis	TVE	Good
5/F/76	CS	ICH	None	SP
Noncavernous sinus				
6/F/49	TS	Tinnitus	None	-
7/F/41	TS	Tinnitus	None	-
8a/M/67	TS	Incidental	TAE	Good
9/M/40	TS	Tinnitus	TVE	Good
10a/F/77	TS	Dementia	TVE	Good
11/F/66	TS	Tinnitus	TAE	Fair
12/F/77	TS and adjacent dura	Tinnitus	SRS	Fair
13/M/60	Dura adjacent to TS	Tinnitus	None	-
8b/M/67	SS	Venous infarct	TVE	Good
10b/F/77	Hypoglossal	Incidental	None	-
14/M/50	CH	Tinnitus	TVE	Good
15/M/48	CH	Tinnitus, dizziness	TVE	Good
16/M/60	CH	Tinnitus	TAE	Fair
17/F/56	SSS	Tinnitus	TAE	Good
18/M/46	SSS	Incidental	None	-
19/M/50	Frontal base	Incidental	None	-
20/M/53	Occipital dura	Tinnitus	TAE	Good
21/M/63	Cerebellar falx	SAH	TAE	Good
22/F/62	Parietosphe- noid osseous-dura	Tinnitus	TVE	Good

Note: Patient 8 and 10 had two dural AVFs (8a and 8b and 10a and 10b, respectively) For patients 8a, 10b, 18, and 19, in the Clinical Manifestation column, incidental means that there were no AVF-associated clinical manifestations, and AVF was detected incidentally when CTA was performed for other diseases. At presentation, patient 18 had transient ischemic attack, and vertebral artery dissection was diagnosed. CS=cavernous sinus, TS=transverse sigmoid sinus, SS=sigmoid sinus, CH=clivo-hypoglossal area, SSS=superior sagittal sinus, ICH=intracerebral hematoma, SAH=subarachnoid hemorrhage, TAE=transarterial embolization, TVE=transvenous embolization, SRS=stereotactic radiosurgery. A fair outcome was defined as partial symptom relief

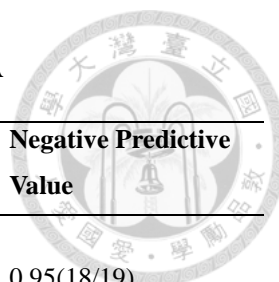
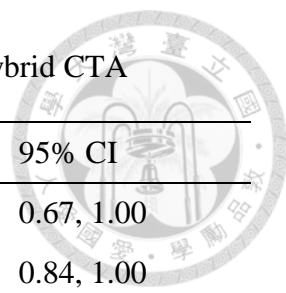


Table 2-2: Diagnostic Performance of Imaging Signs at Hybrid CTA

Imaging Sign	Sensitivity	Specificity	Positive Predictive Value	Negative Predictive Value
Engorged artery				
Value	0.95(19/20)	1.00(18/18)	1.00(19/19)	0.95(18/19)
95% CI	0.75, 1.00	0.85, 1.00	0.85, 1.00	0.74, 1.00
Transosseous enhancing vessels				
Value	0.95(19/20)	0.89(16/18)	0.90(19/21)	0.94(16/17)
95% CI	0.75, 1.00	0.66, 0.98	0.70, 0.99	0.71, 1.00
Engorged extracranial veins				
Value	0.81(13/16)	1.00(22/22)	1.00(13/13)	0.88(22/25)
95% CI	0.56, 0.94	0.87, 1.00	0.80, 1.00	0.90, 1.00
Engorged cortical veins				
Value	1.00(7/7)	1.00(31/31)	1.00(7/7)	1.00(31/31)
95% CI	0.68, 1.00	0.90, 1.00	0.68, 1.00	0.90, 1.00
Asymmetric sinus enhancement				
Value	0.96(23/24)	0.93(13/14)	0.96(23/24)	0.93(13/14)
95% CI	0.78, 1.00	0.66, 1.00	0.78, 1.00	0.66, 1.00
Sinus occlusion				
Value	0.89(8/9)	1.00(29/29)	1.00(8/8)	0.97(29/30)
95% CI	0.54, 1.00	0.90, 1.00	0.71, 1.00	0.82, 1.00
Overall				
Value	0.93(89/96)	0.98(129/132)	0.97(89/92)	0.95(129/136)
95% CI	0.85, 0.97	0.93, 1.00	0.90, 0.99	0.90, 0.98

Note.—Data are for the 22 patients with dural AVFs and 14 control subjects. Numbers in parentheses are numbers of subjects and were used to calculate the values as proportions.

Table 2-3: Interobserver Agreement in Reading Imaging Signs at Hybrid CTA



Imaging Sign	κ Value	95% CI
Engorged artery	0.84	0.67, 1.00
Transosseous enhanced vessels	0.95	0.84, 1.00
Engorged extracranial vein	0.56	0.29, 0.83
Engorged cortical vein	0.92	0.78, 1.00
Asymmetric sinus enhancement	0.94	0.83, 1.00
Dural sinus occlusion	1.00	1.00, 1.00

Table 2-4: Comparison of DSA with Readers for Grades Assigned to 24 Dural AVFs

Region	Location	Grade (Cognard)			Observed Agreement		
		DSA	Reader 1	Reader 2	Between DSA and Reader 1	Between DSA and Reader 2	Between Readers 1 and 2
Cavernous sinus					5/5(100)	5/5(100)	5/5(100)
1	CS	I	I	I			
2	CS	I	I	I			
3	CS	I	I	I			
4	CS	I	I	I			
5	CS	IIA+B	IIA+B	IIA+B			
Transverse sigmoid sinus					7/9(78)	8/9(89)	7/9(78)
6	TS	I	I	I			
7	TS	I	I	I			
8a	TS	I	I	I			
9	TS	IIA	IIA+B	I			
10a	TS	IV	IV	IV			
11	TS	IIA	IIA+B	IIA			
12	TS and adjacent dura	IIA	IIA	IIA			
13	Dura adjacent to TS	IIA	IIA	IIA			
8b	Sigmoid sinus	IV	IV	IV			
Hypoglossal and clival areas					4/4(100)	4/4(100)	4/4(100)
10b	Hypoglossal area	I	I	I			
14	CH	I	I	I			
15	CH	I	I	I			
16	CH	I	I	I			
Superior sagittal sinus					2/2(100)	2/2(100)	2/2(100)
17	SSS	IV	IV	IV			
18	SSS	IV	IV	IV			
Other					4/4(100)	4/4(100)	4/4(100)
19	Frontal base	IV	IV	IV			
20	Occipital dura	IV	IV	IV			
21	Cerebellar falx	IV	IV	IV			
22	Parietospheno- osseous-dura	I	I	I			
Overall					22/24(92)	23/24(96)	22/24(92)

Note: Patients 8 and 10 had two dural AVFs each (8a and 8b and 10a and 10b, respectively). Number in parenthesis is the percentage. CS=cavernous sinus, TS=transverse sigmoid sinus, CH=clival-hypoglossal area, SSS=superior sagittal sinus.

Chapter 3

Predicting Procedure Successful Rate and 1-Year Patency After Endovascular Recanalization for Chronic Carotid Artery Occlusion by CT Angiography



3.1 Introduction

In chronic internal carotid artery (ICA) occlusion, the hemodynamics may be normal, or severely impaired, depending on recruitment of cerebral collaterals [25,26]. When ICA stenosis progresses to occlusion, the reduction of blood supply to the perfused territory is usually compensated by extracranial–intracranial (EC/IC) and intracranial collaterals. In fact, an ICA chronic total occlusion (CTO) bears a considerable risk of ipsilateral ischemic stroke. According to some reports, patients with carotid CTO also have a risk of recurrent stroke of approximately 6.3% [27]. In addition, the risk of recurrent stroke increases to approximately 12% per year in CTO patients who also have compromised hemodynamic status [28,29]. Other researchers have reported a risk of recurrent stroke as high as 86% in a 7-year follow-up study [30]. Furthermore, advanced imaging techniques have uncovered microstructural changes in normal appearing brain tissue in such patients [31]. Such findings have been related to functional disability, higher mortality, and a decline in psychomotor speed, executive functions, and working memory [31].

Over the last few decades, the prevention of secondary stroke in patients with carotid disease has improved with more rigorous control of blood pressure and the introduction of statins combined with anti-platelet therapy [32,33]. Medical treatment

has become the prevailing doctrine in treating carotid CTOs and aggressive treatment of carotid CTOs remains controversial [34]. The carotid occlusion surgery study (COSS) compared the benefit of superficial temporal artery — middle cerebral artery (MCA) bypass vs. medical treatment in preventing stroke in carotid CTO [35]. The 30-day event rate in the surgical group was approximately 14.4% and the 2-year outcome rate did not differ significantly between the surgical (21%) and the medical groups (22.7%), although vessel patency was demonstrated in 90% of patients [35,36].

With the latest advancements in stenting and hybrid-surgical technique, some recent non-randomized studies have shown the feasibility of carotid artery stenting (CAS) and carotid endarterectomy (CEA) in carotid CTO [37-40]. In addition, their results suggest that such interventions might improve neurocognitive function in carotid CTO patients [37-40]. CEA success rates were also shown to differ depending on the ultrasound findings in CTO [39].

The patient selection criteria for the treatment of carotid CTOs are still controversial. In few small-series reports, in acute to chronic ICA occlusion from cervical to petrous segment could be endovascularly recanalized with high successful rates with frequent complication such as subarachnoid hemorrhage (SAH), arterial dissection, symptomatic and asymptomatic embolic events [41-43]. It is rare to find report about how to predict the technical success rates, complication rates, and re-occlusion after endovascular recanalization using non-invasive technique such as CTA. In this study, we retrospectively analyzed the pre-procedural CTA in patients with carotid CTO and its relationship to short-term outcomes including technical success rates, complication rates, and re-occlusion after endovascular recanalization.

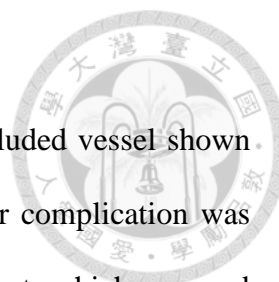
3.2 Materials and Methods



3.2.1 Subjects

This retrospective study was approved by our Institutional Review Board. All medical images and records were analyzed and reviewed. Patients who were diagnosed and confirmed with carotid CTOs by CTA (and who subsequently underwent endovascular recanalization within 3 months of the CTA) were included in the study. The endovascular recanalization was performed at least 2 months after initial diagnosis of carotid occlusion. The exclusion criteria were: (1) acute occlusion of the carotid artery; (2) severe carotid stenosis with string sign on CTA but occlusion on angiography before recanalization; (3) history of previous stenting of the occluded artery; (4) viable head–neck malignancy or prominent radiation necrosis; and (5) severe disabling stroke precluding further recanalization. Hybrid CTA images were used for evaluation. The endovascular recanalization procedure was performed, as previously described [37,38]. The medical conditions, results of the recanalization (success or failure), presence of a major event within 30 days, and patency on follow-up imaging studies were recorded. The patency or re-occlusion was assessed by ultrasound and/or CTA.

Patients were divided into two groups according to the extent of ICA occlusion based on the ICA classification proposed by Bouthillier et al. [44]. In this system, the ICA is divided into seven segments, i.e., C1, cervical; C2, petrous; C3, lacerum; C4, cavernous; C5, clinoid; C6, ophthalmic; and C7, communicating. C5 was used as the landmark, or milestone, to divide the patients into groups A and B. Group A patients had occlusions which involved the ICA up to the clinoid segment and beyond, while group B patients had occlusions which were proximal to the clinoid segment of the ICA or involved only the common carotid artery.



3.2.2 Patient Outcomes

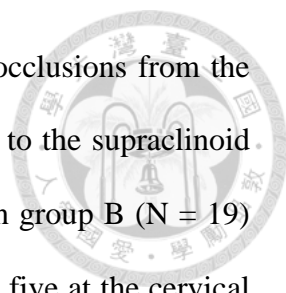
Technical success was defined as complete patency of the occluded vessel shown on immediate post-procedural angiography. A periprocedural major complication was defined as a neurological or cardiovascular event within 30 days. Events which occurred after 30 days were defined as delayed complications. Stent patency was evaluated within 1 year of the recanalization using follow-up CTA or carotid duplex ultrasound. Re-occlusion was defined as no flow shown on the follow-up imaging studies.

3.2.3 Statistical Analysis

All clinical variables were compared between the two groups. The student t-test was used for continuous data and the chi-square test was used for categorical data. A logistic regression model was used to analyze clinical predictors and clinical outcomes. The regression coefficient was analyzed by the Wald test. Multivariable regression and stratified analysis were used to control confounders. The 1-year vascular patency was also analyzed by Kaplan–Meier survival curve analysis. Patients with a follow-up time of ≤ 1 year were considered as right censored. The predictors were compared by Wilcoxon test. The significance level was set at .05. Statistical analyses were conducted using SAS software, version 9.4 (SAS Institute, Inc., Cary, North Carolina).

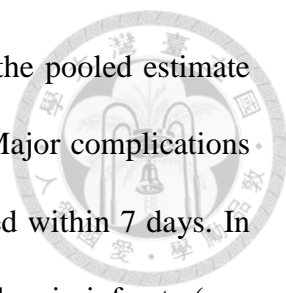
3.3 Results

From January 2008 to July 2015, 41 patients with a total of 42 carotid CTOs were included in the analysis. The one patient with bilateral occlusions was treated in two sessions. Thirty-two CTO arteries (32/42, 76%) in 31 patients were symptomatic (including 23 ipsilateral minor strokes; nine transient ischemic attack). Ten patients (10/41, 24%) had non-specific symptoms such as dizziness, fainting, or neurocognitive



decline. The extent of occlusion in group A (N = 23) included 13 occlusions from the carotid bulb to the clinoid segment of the ICA, eight from the bulb to the supraclinoid ICA, and two from the bulb to the MCA. The extent of occlusion in group B (N = 19) included four occlusions at the common carotid artery (CCA) alone, five at the cervical ICA, five from the bulb to the petrous ICA, and five from the bulb to the cavernous ICA (**Figure 3-1**).

In total, 29 arteries (29/42, 69%) were successfully recanalized. One patient (who failed revascularization) had an acute SAH during the procedure, while the other 12 patients with failed recanalizations had no acute or new onset of symptoms. The technical success rate was 52% (12/23) in group A and 89% (17/19) in group B. The major complication rate in group A was 22% (5/23) and 0 in group B. The 1-year reocclusion rate was 92% (11/12) in group A and 0 in group B. One patient was lost to follow-up after successful recanalization in group B. When comparing group A with group B, technical success rate ($P = 0.0093$) and stent patency ($P = 0.001$) were significantly different (**Table 3-1**). Based on univariable logistic regression analysis of technical success, group B had a higher success rate than group A (odds ratio: 7.79; CI: 1.45–41.73; $P = 0.0165$). Since diabetes was a possible confounder, it was used to adjust the logistic regression model. The group effect was still significant based on multivariable logistic regression (odds ratio: 12.71; CI: 2.06–78.44; $P = 0.0062$). Analysis of stent patency was performed in 28 patients who were successfully recanalized. Chi-square tests showed that the group effect ($P=0.001$) and diabetes ($P=0.004$) were associated with stent occlusion (**Table 3-2**). Stratified analysis showed that the group effect was significant in diabetic patients (odds ratio: 75.00; CI: 1.16–4868.64; $P = 0.0027$) and non-diabetic patients (odds ratio: 87.00; CI:

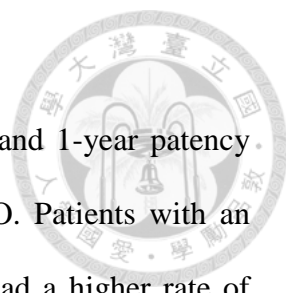


2.99–2531.93; $P = 0.0002$). However, the odds ratio was lower in the pooled estimate (corrected Mantel Haenszel odds ratio: 82.05; CI: 5.96–1129.50). Major complications occurred in five patients in group A (5/23, 21.7%) and four occurred within 7 days. In group A, there was one subarachnoid hemorrhage (SAH), three ischemic infarcts (one immediate post-procedure and two acute in-stent thromboses on the 1st day and 5th day, respectively) and one delayed stroke (1/23, 4.3 due to stent occlusion on the 40th day. Two patients died (one SAH and one acute in-stent thrombosis). Other 3 had good recovery. No immediate or delayed major complication or death occurred in group B.

On the follow-up images within 1 year, of the 29 successfully recanalized arteries, 17 arteries (one in group A; 16 in group B) were patent, 11 (11 in group A; 0 in group B) were occluded, and one had no follow-up imaging. In group A, the only patent artery was followed-up for only 2 months after recanalization. In group B, five arteries were patent on the follow-up images performed within 8 months.

Based on survival analysis of stent occlusion at one-year follow-up, of the 28 subjects deemed technically successes, six subjects with <1 year of follow-up were considered right-censored. One patient was excluded due to loss of follow-up after successful procedure. Eleven occlusion events, all in group A, were recorded. The median time of re-occlusion was 4 months (95% CI: 1–7 months). Based on univariable analysis of the clinical predictors, only the group effect was significant ($P < 0.0001$) by Wilcoxon test (**Table 3-3**). The Kaplan–Meier survival curve for groups A and B is shown in **Figure 3-2**.

3.4 Discussion



Our results showed that CTA can predict the successful rate and 1-year patency rate after endovascular recanalization in patients with carotid CTO. Patients with an occlusion proximal to the clinoid segment of the ICA (group B) had a higher rate of successful recanalization, fewer periprocedural major complications, and better 1-year patency rates as compared with those patients whose occlusions were located at, or distal to, the clinoid segment of the ICA (group A). The group B result is consistent with other small-number series [41,42]; however, group A result has never been reported. This might be a result of reporting bias since failure cases were not reported. Compared with group A, our group B patients had a higher technical success rate (89%), no periprocedural complications, and no re-occlusions within one year. Only a few studies have shown the feasibility of CAS and CEA in carotid CTO [37-40], and their reported successful rates were usually lower than in treating patients with carotid stenosis. Since our group A patients had higher rates of technical failure (48%), periprocedural complications (22%), and re-occlusion within one year (92%), this would effectively cancel out the overall benefit of recanalization for carotid CTO if we analyzed both patient groups together. Appropriate patient selection for recanalization of carotid CTOs can demonstrate the benefit of such an invasive procedure over medical management. The results of our study suggest that patients with carotid CTOs that are proximal to the level of clinoid segment of the ICA on CTA are more appropriate candidates for recanalization.

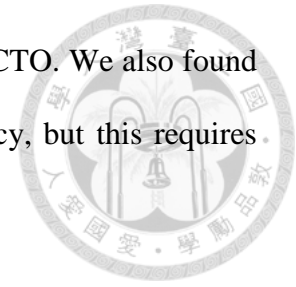
The underlying reason for selecting the clinoid segment of the ICA as the milestone for successful recanalization in carotid CTO is unclear but it may be related to local ICA anatomic structure. The clinoid segment is located between the proximal

dural ring and the distal dural ring. The ICA becomes intradural after the distal dural ring [44]. The distal dural ring is a complete ring that entirely surrounds the ICA and fuses laterally with the adventitia of the ICA. We speculate that the relatively stronger tightening effort by the distal dural ring may be responsible for preventing successful recanalization beyond this point.

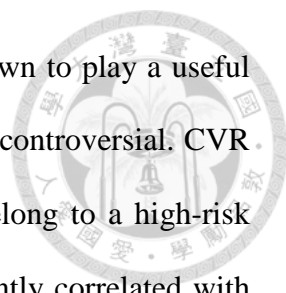
A recent report has mentioned that MR angiography and CTA may overestimate the presence of an ICA occlusion due to false-positive findings [45]. However, all cases in our study were confirmed as CTOs during the endovascular procedure that was later performed.

Ultrasound studies have been used to predict the success rates of CEA in carotid CTO [39]. Two series have shown that 60% and 80% of ICA occlusions, respectively, had some degree of EC/IC collaterals [30,46]. The ipsilateral ophthalmic artery has been considered an important EC/IC collateral in ICA occlusion or severe stenosis [46-48]. We found good outcomes in 89.5% of the 19 patients with patent collaterals from the ophthalmic artery to the ICA in group B. However, the outcomes in a subgroup (occlusion from bulb to clinoid segment) of 13 patients in group A were still poor. Although these 13 patients had ophthalmic artery collaterals, the technical success rate (54.8%, 7/13) was low, the complication rate (23.0%, 3/13) was high, and the re-occlusion rate (85.7%, 6/7) within 1 year was high. This indicates that the ophthalmic artery collateral is not a major factor in predicting outcomes after endovascular recanalization in carotid CTO. In our series, all group A patients had relatively long occluded segments, i.e., their segments extended from the carotid bulb to the ophthalmic artery orifice and beyond. We speculate that the longer the occluded

segment, the poorer the outcome after recanalization of the carotid CTO. We also found that diabetes was a probable clinical predictor of short-term patency, but this requires further validation.



Our study had several limitations including its retrospective nature and the lack of regular angiographic follow-up. Using either ultrasound or CTA, we could not identify mild to moderate re-stenosis which might have existed before occlusion. The higher censored rate potentially resulted in an overestimation of favorable outcomes in the group B patients. Patients without clinical events might have been less intensively followed-up. However, in our non-parametric survival analysis, the results were still valid even when the occlusive event occurred in the group B patient at the time of censoring. In this study, we only analyzed the anatomic differences between the two groups, and other factors (such as the length of time the vessel was occluded or the hemodynamic status) were not evaluated. Patients probably had longer occlusion times in group A, causing higher technical failure rates and more complications. However, accurate measurements of the length of time the vessel was occluded was not possible in the current study, since we had no data regarding the date the vessel began to occlude. We presume that the longer the occlusion time and the longer the occluded segment, the harder the thrombus becomes. It is more difficult to recanalize a vessel with chronic thrombi compared with fresh thrombi (as has been noted in the recanalization of acute occlusion of major vessels). Clinically, evaluation of cerebral hemodynamic status involves assessment of cerebral vascular reserve (CVR) which provides information on cerebral autoregulation and collateral circulation [49]. CVR is defined as a shift between cerebral blood flow and cerebral blood flow velocity before and after administration of a potent vasodilatory stimulus such as acetazolamide (Diamox) or 8%



CO₂ inhalation. In patients with carotid CTOs, CVR has been shown to play a useful role in patient selection. However, the data from different papers is controversial. CVR may identify asymptomatic patients with carotid occlusion who belong to a high-risk subgroup for ischemic stroke [50]. An impaired CVR has significantly correlated with ipsilateral ischemic stroke. In asymptomatic carotid CTO patients, the annual ipsilateral ischemic event risk was 1.8% in patients with good CVRs compared with 7.1% in patients with impaired CVRs. In symptomatic patients, the annual risk of stroke in patients with symptomatic carotid CTO was 3–6% in patients with good CVRs compared with 10–17% in patients with impaired CVRs [51-53]. However, others have reported that reduced CVR plays no major role in stroke recurrence among symptomatic patients [54, 55]. Moreover, spontaneous improvement in CVR has been demonstrated during the first few months after ICA occlusion [56, 57]. We suggest that a CVR study might be useful in symptomatic patient selection when considering recanalization in the presence of carotid CTO. Endovascular recanalization, such as stenting, should be performed after CTA and should target patients with occluded ICAs proximal to the clinoid segment.

3.5 Conclusion

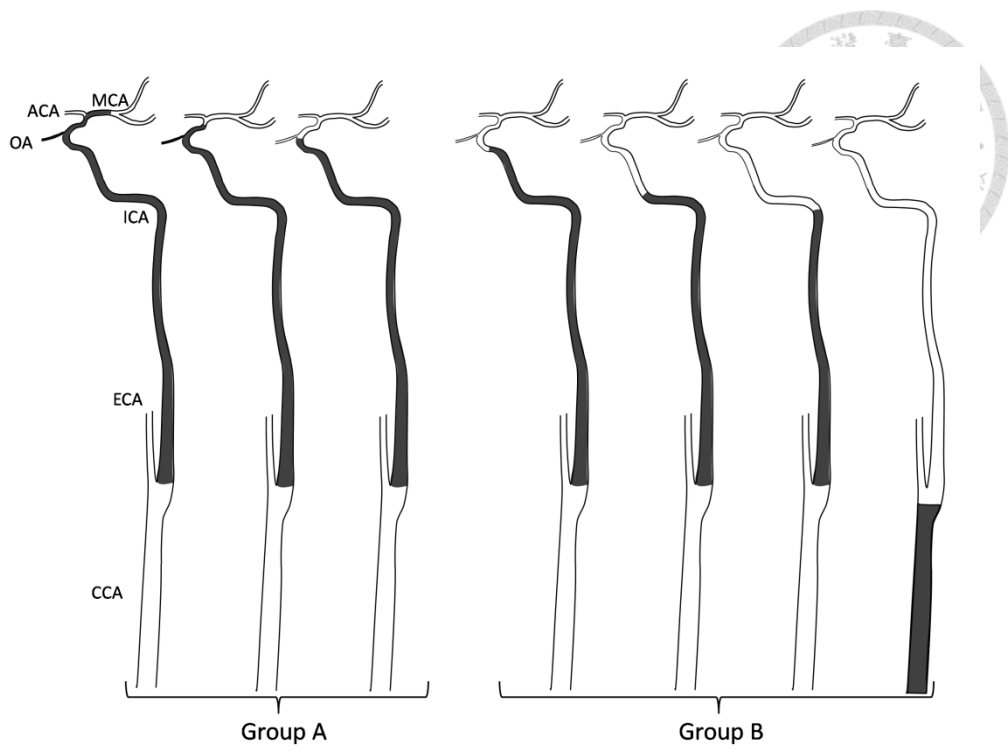
CTA may play a role in patient selection and may predict successful rate and 1-year patency after endovascular recanalization in patients with carotid CTOs. Patients with occlusions proximal to the clinoid segment of the ICA had a higher success rate after recanalization, less periprocedural major complications, and better patency rates as compared with those whose occlusion was located at, or distal to, the clinoid segment of the ICA.

Note:

This part was published on *Internal Journal of Cardiology* 2016.

Lee CW, Lin YH, Liu HM, Wang YF, Chen YF, Wang JL. Predicting procedure successful rate and 1-year patency after endovascular recanalization for chronic carotid artery occlusion by CT angiography. *International Journal of Cardiology*. 2016 Jul 9;221:772-776.





	Group A			Group B			
Case number (n)	2	8	13	5	5	5	4
Technical success (n)	0	5	7	4	4	5	4
Major complication (n)	0	2	3	0	0	0	0
Re-occlusion within 1 year (n)	/	5	6	0	0	0	0

Figure 3-1: Sub-classification of the 42 carotid chronic total occlusions in 41 patients and their outcomes.

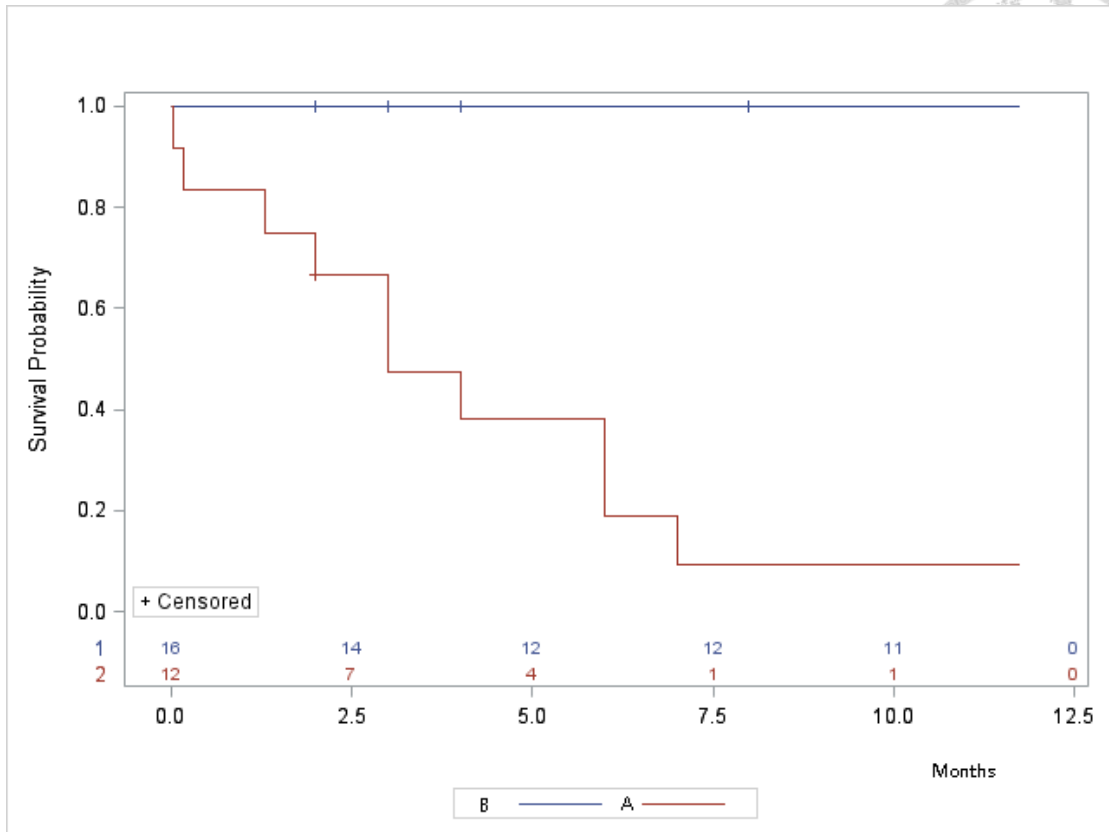
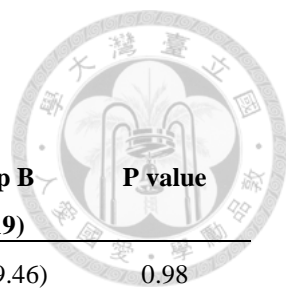



Figure 3-2: Kaplan-Meier Product Limit survival functional estimates for group A (red) and group B (blue) patients after endovascular recanalization for chronic carotid artery occlusion.

Table 3-1: Demographics and clinical characteristics of all patients.

Variable	Total (N=42)	Group A (N=23)	Group B (N=19)	P value
Age – yrs (SD)	65.45(9.96)	65.48(10.57)	65.42(9.46)	0.98
Male gender – no. (%)	34(81)	17(74)	17(89)	0.20
Right side –no. (%)	19(45)	11(48)	8(42)	0.71
Successful – no. (%)	29 (69)	12(52)	17(89)	0.0093**
Major complication – no. (%)	5(12)	5(22)	0(0)	0.03*
Patency (N=28) – no. (%)	17(61)	1(8)	16(100)	<0.0001**
Stent number (N=29) – no. (SD)	2.25(1.40)	2.42(1.56)	2.12(1.31)	0.60
Symptomatic – no. (%)	32(76)	17(74)	15(79)	0.70
Coronary heart disease – no. (%)	26(62)	13(57)	13(68)	0.43
Diabetes – no. (%)	12(29)	10(43)	2(11)	0.0186*
Hypertension – no. (%)	32(76)	18(78)	14(74)	0.73
Hyperlipidemia – no. (%)	25(60)	13(56)	12(63)	0.66
Cancer – no. (%)	9(21)	4(17)	5(26)	0.48
Smoking – no. (%)	17(40)	9(39)	8(42)	0.85

The P-value was obtained using the chi-square test for categorical data, and the t-test for continuous data.

Table 3-2: Odds ratio for clinical predictors of stent occlusion in technically successful patients (N = 28).



Variable	Odds ratio (CI)	P-value
Group effect	253.00(9.44-6777.47)	<0.001**
Old age (age > 55)	0.36(0.049-2.59)	0.30
Male gender	0.60(0.072-5.03)	0.64
Right side	0.94(0.21-4.29)	0.93
Symptomatic	1.11(0.21-6.01)	0.90
Coronary heart disease	0.73(0.15-3.65)	0.70
Diabetes	13.13(1.92-89.52)	0.004*
Hypertension	1.88(0.29-11.97)	0.50
Hyperlipidemia	1.87(0.37-9.63)	0.45
Cancer	0.24(0.02-2.41)	0.20
Smoking	2.00(0.41-9.71)	0.39

The P-values were obtained by chi-square test.

Table 3-3: Univariable non-parametric survival analysis of clinical predictors for one-year stent patency.



Variable	P-value
Group effect	<0.001**
Old age (age > 5)	0.8258
Gender	0.5457
Right side	0.8389
Diabetes	0.0553
Coronary heart disease	0.3141
Hypertension	0.8723
Symptomatic	0.7853
Hyperlipidemia	0.3572
Smoking	0.4119
Cancer	0.3895

Note: Wilcoxon test was used.

Chapter 4

Future Work



Hybrid CTA provides an opportunity for more accurate detection and diagnosis of vascular diseases in head and neck. It can potentially be used in diseases other than dural arteriovenous fistula and carotid occlusion, and may improve visualization and 3D reconstruction of vessels after successful bone removal.

Rapid processing software is required for quick and accurate diagnosis in emergent situations. The prototype software has to be converted into robust software, so that the usage can be easier and more popular.

For vascular lesions in or near the bones, computer-assisted detection (CAD) is potentially difficult. After successful removal of bone and calcification by hybrid subtraction, CAD of vascular lesions can be done easier since there is no need for segmentation. Vascular caliber analysis can also be done easily. Preservation of image quality away from bones in hybrid CTA would not affect the performance of CAD in non-bone area.

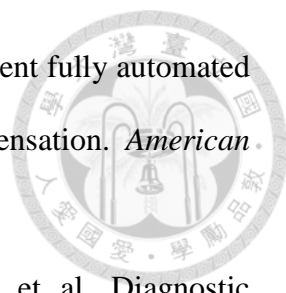
Dual-energy CT is also a good tool for bone removal in CTA [59, 60]. However, there is still no study comparing the image quality and radiation dose between subtraction CTA and dual-energy CTA. With satisfactory registration and hybrid subtraction, CTA done by simple multi-detector row CT is still valuable since it is more widely used. Not all cases can receive dual-energy CTA. A bone removal technique for

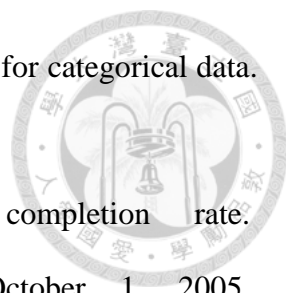
usual CT scanner is still required. After establishment of dual-energy CT, further comparison can be implemented.

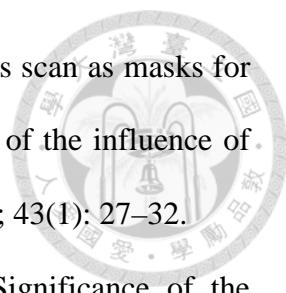


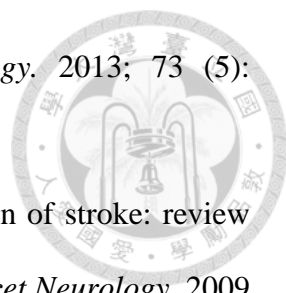
References

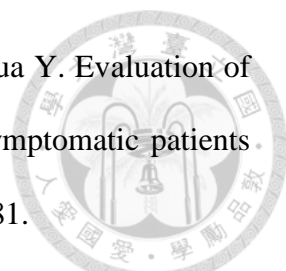
1. Cloft HJ, Joseph GJ, Dion JE. Risk of cerebral angiography in patients with subarachnoid hemorrhage, cerebral aneurysm, and arteriovenous malformation: a meta-analysis. *Stroke* 1999; 30(2):317–320.
2. Willinsky RA, Taylor SM, TerBrugge K, Farb RI, Tomlinson G, Montanera W. Neurologic complications of cerebral angiography: prospective analysis of 2,899 procedures and review of the literature. *Radiology* 2003; 227 (2): 522 – 528.
3. Tipper G, U-King-Im JM, Price SJ, et al. Detection and evaluation of intracranial aneurysms with 16-row multislice CTA. *Clinical Radiology*. 2005; 60 (5): 565 – 572.
4. Chappell ET, Moure FC, Good MC. Comparison of computed tomographic angiography with digital subtraction angiography in the diagnosis of cerebral aneurysms: a metaanalysis. *Neurosurgery* 2003; 52 (3): 624 – 631; discussion 630–631.
5. Hashimoto H, Iida J, Hironaka Y, Okada M, Sakaki T. Use of spiral computerized tomography angiography in patients with subarachnoid hemorrhage in whom subtraction angiography did not reveal cerebral aneurysms. *Journal of Neurosurgery*. 2000; 92 (2): 278 – 283.
6. Koelemay MJ, Nederkoorn PJ, Reitsma JB, Majoie CB. Systematic review of computed tomographic angiography for assessment of carotid artery disease. *Stroke* 2004; 35 (10): 2306 – 2312.
7. Josephson SA, Bryant SO, Mak HK, Johnston SC, Dillon WP, Smith WS. Evaluation of carotid stenosis using CTA in the initial evaluation of stroke and TIA. *Neurology* 2004 ; 63 (3): 457 – 460.
8. Lell MM, Ditt H, Panknin C, Sayre JW, Ruehm SG, Klotz E, Tomandl BF,

- 
- Villablanca JP. Bone-subtraction CTA: evaluation of two different fully automated image registration of procedures for interscan motion compensation. *American Journal of Neuroradiology*. 2007 ; 28 (7): 1362 – 1368.
9. Romijn M, Gratama van Andel HA, van Walderveen MA, et al. Diagnostic accuracy of CTA with matched mask bone elimination for detection of intracranial aneurysms: comparison with digital subtraction angiography and 3D rotational angiography. *American Journal of Neuroradiology*. 2008; 29 (1): 134 – 139
 10. Gonzalez RC, Woods RE. Digital image processing. Reading, Mass: Addison-Wesley, 1992 ; 518 – 524.
 11. Venema HW, Hulsmans FJH, den Heeten GJ. CTA of the circle of Willis and intracranial internal carotid arteries: maximum intensity projection with matched mask bone elimination—feasibility study. *Radiology*. 2001; 218 (3): 893 – 898.
 12. De Marco JK, Dillon WP, Halback VV, Tsuruda JS. Dural arteriovenous fistulas: evaluation with MR imaging. *Radiology* 1990; 175 (1): 193 – 199.
 13. Noguchi K, Melhem ER, Kanazawa T, Kubo M, Kuwayama N, Seto H. Intracranial dural arteriovenous fistulas: evaluation with combined 3D time-of-flight MR angiography and MR digital subtraction angiography. *American Journal of Roentgenology*. 2004; 182 (1): 183 – 190.
 14. Horie N, Morikawa M, Kitigawa N, Tsutsumi K, Kaminogo M, Nagata I. 2D Thick-section MR digital subtraction angiography for the assessment of dural arteriovenous fistulas. *American Journal of Neuroradiology*. 2006; 27 (2): 264–269.
 15. Cognard C, Gobin YP, Pierot L, et al. Cerebral dural arteriovenous fistulas: clinical and angiographic correlation with a revised classification of venous drainage. *Radiology* 1995; 194 (3):671–680.

- 
16. Landis JR, Koch GG. The measurement of observer agreement for categorical data. *Biometrics* 1977; 33 (1): 159–174.
17. Sauro J. Confidence interval calculator for a completion rate. <http://www.measuring-usability.com/wald.htm>. Published October 1, 2005. Accessed September 2, 2009.
18. Lowry R. Cohen's unweighted kappa, kappa with linear weighting, kappa with quadratic weighting, frequencies and proportions of agreement. <http://faculty.vassar.edu/lowry/kappa.html>. Accessed September 2, 2009.
19. Cohen SD, Goins JL, Butler SG, Morris PP, Browne JD. Dural arteriovenous fistula: diagnosis, treatment, and outcomes. *Laryngoscope* 2009; 119 (2):293 – 297.
20. Tsai LK, Jeng JS, Liu HM, Wang HJ, Yip PK. Intracranial dural arteriovenous fistulas with or without cerebral sinus thrombosis: analysis of 69 patients. *Journal of Neurology, Neurosurgery, and Psychiatry*. 2004; 75 (11):1639–1641.
21. Klisch J, Huppertz HJ, Spetzger U, Hetzel A, Seeger W, Schumacher M. Transvenous treatment of carotid cavernous and dural arteriovenous fistulae: results for 31 patients and review of the literature. *Neurosurgery* 2003; 53 (4): 836 – 856, discussion 856–857.
22. Borden JA, Wu JK, Shucart WA. A proposed classification for spinal and cranial dural arteriovenous fistulous malformations and implications for treatment. *Journal of Neurosurgery*. 1995; 82 (2):166–179.
23. Takahashi S, Tomura N, Watarai J, Mizoi K, Manabe H. Dural arteriovenous fistula of the cavernous sinus with venous congestion of the brain stem: report of two cases. *American Journal of Neuroradiology*. 1999; 20 (5): 886–888.
24. Lell MM, Ditt H, Panknin C, Sayre JW, Klotz E, Ruehm SG, Villablanca JP.

- 
- Cervical CTA comparing routine non-contrast and a late venous scan as masks for automated bone subtraction: feasibility study and examination of the influence of patient motion on image quality. *Investigative Radiology*. 2008 ; 43(1): 27–32.
25. Surikova I, Meisel S, Siebler M, Wittsack HJ, Seitz RJ. Significance of the perfusion–diffusion mismatch in chronic cerebral ischemia. *Journal of Magnetic Resonance Imaging*. 2006; 24: 771–778.
 26. Liebeskind DS, Cotsonis GA, Saver JL, Lynn MJ, Turan TN, Cloft HJ, Chimowitz MI; Warfarin-Aspirin Symptomatic Intracranial Disease (WASID) Investigators. Collaterals dramatically alter stroke risk in intracranial atherosclerosis. *Annals of Neurology*. 2011; 69 (6): 963–974.
 27. Klijn CJ, Kappelle LJ, Algra A, van Gijn J. Outcome in patients with symptomatic occlusion of the internal carotid artery or intracranial arterial lesions: a meta-analysis of the role of baseline characteristics and type of antithrombotic treatment. *Cerebrovascular Diseases*. 2001; 12: 228–234.
 28. Klijn CJ, Kappelle LJ, Tulleken CA, van Gijn J. Symptomatic carotid artery occlusion. A reappraisal of hemodynamic factors. *Stroke*. 1997; 28: 2084–2093.
 29. Persoon S, Luitse MJ, de Borst GJ, van der Zwan A, Algra A, Kappelle LJ, Klijn CJ. Symptomatic internal carotid artery occlusion: a long-term follow-up study, *Journal of Neurology, Neurosurgery, and Psychiatry*. 2011; 82 (5):521–526.
 30. Bryan DS, Carson J, Hall H, He Q, Qato K, Lozanski L, McCormick S, Skelly CL. Natural history of carotid artery occlusion. *Annals of Vascular Surgery*. 2013; 27 (2): 186–193.
 31. Jokinen H, Schmidt R, Ropele S, Fazekas F, Gouw AA, Barkhof F, Scheltens P, Madureira S, Verdelho A, Ferro JM, Wallin A, Poggesi A, Inzitari D, Pantoni L, Erkinjuntti T; LADIS Study Group. Diffusion changes predict cognitive and

- 
- functional outcome: the LADIS study. *Annals of Neurology*. 2013; 73 (5): 576–583.
32. Amarenco P, Labreuche J. Lipid management in the prevention of stroke: review and updated meta-analysis of statins for stroke prevention. *Lancet Neurology*. 2009 8: 453–463.
33. The Esprit study group, Aspirin plus dipyridamole versus aspirin alone after cerebral ischaemia of arterial origin (ESPRIT): randomised controlled trial. *Lancet* 2006; 367:1665–1673.
34. Issawi A, Klopfenstein J. Can a closed carotid artery be reopened? *Current Cardiology Reports*. 2015; 17 (10): 85.
35. Grubb RL Jr, Powers WJ, Clarke WR, Videen TO, Adams HP Jr, Derdeyn CP; Carotid occlusion surgery study investigators. Surgical results of the carotid occlusion surgery study. *Journal of Neurosurgery*. 2013; 118 (1): 25–33.
36. Reynolds MR, Grubb RL Jr, Clarke WR, Powers WJ, Zipfel GJ, Adams HP Jr, Derdeyn CP; Carotid Occlusion Surgery Study Investigators. Carotid occlusion surgery study investigators. Investigating the mechanisms of perioperative ischemic stroke in the carotid occlusion surgery study. *Journal of Neurosurgery*. 2013; 119 (4): 988–995.
37. Lin MS, Chiu MJ, Wu YW, Huang CC, Chao CC, Chen YH, Lin HJ, Li HY, Chen YF, Lin LC, Liu YB, Chao CL, Tseng WY, Chen MF, Kao HL. Neurocognitive improvement after carotid artery stenting in patients with chronic internal carotid artery occlusion and cerebral ischemia. *Stroke*. 2011 Oct;42(10):2850-4.
38. Kao HL, Lin MS, Wang CS, Lin YH, Lin LC, Chao CL, Jeng JS, Yip PK, Chen SC. Feasibility of endovascular recanalization for symptomatic cervical internal carotid artery occlusion. *J. Am. Coll. Cardiol*. 2007; 49 (7): 765–771.

- 
39. Liu Y, Jia L, Liu B, Meng X, Yang J, Li J, Zhou Y, Jiao L, Hua Y. Evaluation of endarterectomy recanalization under ultrasound guidance in symptomatic patients with carotid artery occlusion, *PLoS One* 2015; 10 (12): e0144381.
40. Shih YT, Chen WH, Lee WL, Lee HT, Shen CC, Tsuei YS. Hybrid surgery for symptomatic chronic total occlusion of carotid artery: a technical note, *Neurosurgery* 2013; 73 (1 Suppl. Operative): (onsE117–23; discussion onsE123).
41. Terada T, Okada H, Nanto M, Shintani A, Yoshimura R, Kakishita K, Masuo O, Matsumoto H, Itakura T, Ohshima K, Yamaga H. Endovascular recanalization of the completely occluded internal carotid artery using a flow reversal system at the subacute to chronic stage. *Journal of Neurosurgery*. 2010; 112 (3): 563–571.
42. Shojima M, Nemoto S, Morita A, Miyata T, Namba K, Tanaka Y, Watanabe E. Protected endovascular revascularization of subacute and chronic total occlusion of the internal carotid artery. *American Journal of Neuroradiology*. 2010; 31 (3): 481–486.
43. Park S, Park ES, Kwak JH, Lee DG, Suh DC, Kwon SU, Lee DH. Endovascular management of long-segmental petrocavernous internal carotid artery (carotid S) occlusion. *Journal of Stroke*. 2015; 17 (3): 336–343.
44. Bouthillier A, van Loveren HR, Keller JT. Segments of the internal carotid artery: a new classification. *Neurosurgery* 1996; 38: 425–433.
45. Marquering HA, Nederkoorn PJ, Beenen LF, Lycklama à Nijeholt GJ, van den Berg R, Roos YB, Majoie CB. Carotid pseudo-occlusion on CTA in patients with acute ischemic stroke: a concerning observation. *Clinical Neurology and Neurosurgery*. 2013; 115 (9): 1591–1594.
46. van Laar PJ, van der Grond J, Bremmer JP, Klijn CJ, Hendrikse J. Assessment of the contribution of the external carotid artery to brain perfusion in patients with

- internal carotid artery occlusion. *Stroke* 2008; 39 (11): 3003–3008.
47. Macchi C, Molino Lova R, Miniati B, Zito A, Catini C, Gulisano M, Pratesi C, Conti AA, Gensini GF. Collateral circulation in internal carotid artery occlusion. A study by duplex scan and magnetic resonance angiography. *Minerva Cardioangiologica*. 2002; 50 (6): 695–700.
48. Henderson RD, Eliasziw M, Fox AJ, Rothwell PM, Barnett HJ. Angiographically defined collateral circulation and risk of stroke in patients with severe carotid artery stenosis. North American Symptomatic Carotid Endarterectomy Trial (NASCET) group. *Stroke* 2000; 31 (1): 128–132.
49. Dahl A, Russel D, Nyberg-Hansen R, Rootwelt K, Bakke SJ. Cerebral vasoreactivity in unilateral carotid artery disease. A comparison of blood flow velocity and regional cerebral blood flow measurements. *Stroke* 1994; 25: 621–626.
50. Kimiagar I, Bass A, Rabey JM, Bornstein NM, Gur AY. Long-term follow-up of patients with asymptomatic occlusion of the internal carotid artery with good and impaired cerebral vasomotor reactivity. *European Journal of Neurology*. 2010; 17: 1285–1290.
51. Vernieri F, Pasqualetti P, Passarelli F, Rossini PM, Silvestrini M. Outcome of carotid artery occlusion is predicted by cerebrovascular reactivity. *Stroke* 1999; 30: 593–598.
52. Vernieri F, Pasqualetti P, Matteis M, Passarelli F, Troisi E, Rossini PM, Caltagirone C, Silvestrini M. Effect of collateral blood flow and cerebral vasomotor reactivity on the outcome of carotid artery occlusion. *Stroke* 2001; 32: 1552–1558.
53. Ogasawara K, Ogawa A, Yoshimoto T. Cerebrovascular reactivity to

acetazolamide and outcome in patients with symptomatic internal carotid or middle cerebral artery occlusion. A xenon-133 single-photon emission computed tomography study. *Stroke*. 2002; 33: 1857–1862.

54. Yokota C, Hasegawa Y, Minematsu K, Yamaguchi T. Effect of acetazolamide reactivity on long-term outcome in patients with major cerebral artery occlusive diseases. *Stroke*. 1998; 29: 640–644.
55. Zbornikova V. Long term follow-up of unilateral occlusion of the internal carotid artery including repeated tests of vasomotor reactivity by transcranial Doppler. *Neurological Research*. 2006; 28: 220–224.
56. Widder B, Kleiser B, Krapf H. Course of cerebrovascular reactivity in patients with carotid artery occlusion. *Stroke*. 1994; 25: 1963–1967.
57. Cao B, Hasegawa Y, Yokota C, Minematsu K, Yamaguchi T. Spontaneous improvement in reduced vasodilatory capacity in major cerebral arterial occlusive disease. *Neuroradiology* 2000; 42: 19–25
58. Li Q, Lv F, Wei Y, Luo T, Xie P. Automated subtraction CT angiography for visualization of the whole brain vasculature: a feasibility study. *Academic Radiology*. 2013 Aug; 20(8): 1009-14.
59. Postma AA, Das M, Stadler AA, Wildberger JE. Dual-Energy CT: What the Neuroradiologist Should Know. *Current Radiology Reports*. 2015; 3(5): 16.